of *CHRNA1* compromises expression of the α1 subunit in thymic epithelial cells, and increases the chance of developing myasthenia gravis.

Acknowledgements

Works in our laboratories were supported by Grants-in-Aid from the MEXT and the MHLW of Japan (to K.O.), and by the NIH grant (NS6277) and the Muscular Dystrophy Association grant (to A.G.E.).

References

1. Ohno, K., Hutchinson, D.O., Milone, M., Brengman, J.M., Bouzat, C., Sine, S.M. and Engel, A.G. 1995, Proc. Natl. Acad. Sci. U. S. A., 92, 758.
2. Sine, S.M., Ohno, K., Bouzat, C., Auerbach, A., Milone, M., Pruitt, J.N. and Engel, A.G. 1995, Neuron, 15, 229.
3. Ohno, K., Engel, A.G., Shen, X.-M., Selcen, D., Brengman, J., Harper, C.M., Tsujino, A. and Milone, M. 2002, Am. J. Hum. Genet., 70, 875.
4. Milone, M., Shen, X.M., Selcen, D., Ohno, K., Brengman, J., Iannaccone, S.T., Harper, C.M. and Engel, A.G. 2009, Neurology, 73, 228.
5. Huze, C., Bauche, S., Richard, P., Chevessier, F., Goillot, E., Gaudon, K., Ben Ammar, A., Chaboud, A., Grosjean, I., Lecuyer, H.A., Bernard, V., Rouche, A., Alexandri, N., Kuntzer, T., Fardeau, M., Fournier, E., Brancaccio, A., Ruegg, M.A., Koenig, J., Eymard, B., Schaeffer, L. and Hantai, D. 2009, Am. J. Hum. Genet., 85, 155.
6. Chevessier, F., Faraut, B., Ravel-Chapuis, A., Richard, P., Gaudon, K., Bauche, S., Prioleau, C., Herbst, R., Goillot, E., Ioos, C., Azulay, J.P., Attarian, S., Leroy, J.P., Fournier, E., Legay, C., Schaeffer, L., Koenig, J., Fardeau, M., Eymard, B., Pouget, J. and Hantai, D. 2004, Hum. Mol. Genet., 13, 3229.
7. Chevessier, F., Girard, E., Molgo, J., Bartling, S., Koenig, J., Hantai, D. and Witzemann, V. 2008, Hum. Mol. Genet., 17, 3577.
8. Beeson, D., Higuchi, O., Palace, J., Cossins, J., Spearman, H., Maxwell, S., Newsom-Davis, J., Burke, G., Fawcett, P., Motomura, M., Muller, J.S., Lochmuller, H., Slater, C., Vincent, A. and Yamanashi, Y. 2006, Science, 313, 1975.
9. Hamuro, J., Higuchi, O., Okada, K., Ueno, M., Iemura, S., Natsume, T., Spearman, H., Beeson, D. and Yamanashi, Y. 2008, J. Biol. Chem., 283, 5518.
10. Tsujino, A., Maertens, C., Ohno, K., Shen, X.-M., Fukuda, T., Harper, C.M., Cannon, S.C. and Engel, A.G. 2003, Proc. Natl. Acad. Sci. U. S. A., 100, 7377.
11. Ohno, K., Brengman, J., Tsujino, A. and Engel, A.G. 1998, Proc. Natl. Acad. Sci. U. S. A., 95, 9654.
12. Ohno, K., Brengman, J.M., Felice, K.J., Cornblath, D.R. and Engel, A.G. 1999, Am. J. Hum. Genet., 65, 635.
13. Kimbell, L.M., Ohno, K., Engel, A.G. and Rotundo, R.L. 2004, J. Biol. Chem., 279, 10997.
14. Ohno, K., Tsujino, A., Brengman, J.M., Harper, C.M., Bajzer, Z., Udd, B., Beyring, R., Robb, S., Kirkham, F.J. and Engel, A.G. 2001, Proc. Natl. Acad. Sci. U. S. A., 98, 2017.
15. Lang, B. and Vincent, A. 2009, Curr. Opin. Pharm., 9, 336.
16. Hoch, W., McConville, J., Helms, S., Newsom-Davis, J., Melms, A. and Vincent, A. 2001, Nat. Med., 7, 365.
17. Cole, R.N., Reddel, S.W., Gervasio, O.L. and Phillips, W.D. 2008, Ann. Neurol., 63, 782.
18. Higuchi, O., Hamuro, J., Motomura, M. and Yamanashi, Y. in press, Ann. Neurol. (http://onlinelibrary.wiley.com/doi/10.1002/ana.22312/pdf)
19. Keramidas, A., Moorhouse, A.J., Schofield, P.R. and Barry, P.H. 2004, Prog. Biophys. Mol. Biol., 86, 161.
20. Mihailescu, S. and Drucker-Colin, R. 2000, Arch. Med. Res., 31, 131.

21. Mishina, M., Takai, T., Imoto, K., Noda, M., Takahashi, T., Numa, S., Methfessel, C. and Sakmann, B. 1986, Nature, 321, 406.
22. Lee, W.Y., Free, C.R. and Sine, S.M. 2009, J. Neurosci., 29, 3189.
23. Mukhtasimova, N., Lee, W.Y., Wang, H.L. and Sine, S.M. 2009, Nature,
24. Ohno, K., Anlar, B. and Engel, A.G. 1999, Neuromuscul. Disord., 9, 131.
25. Ohno, K., Quiram, P.A., Milone, M., Wang, H.-L., Harper, M.C., Pruitt, J.N., 2nd, Brengman, J.M., Pao, L., Fischbeck, K.H., Crawford, T.O., Sine, S.M. and Engel, A.G. 1997, Hum. Mol. Genet., 6, 753.
26. Engel, A.G., Ohno, K., Bouzat, C., Sine, S.M. and Griggs, R.C. 1996, Ann. Neurol., 40, 810.
27. Michalk, A., Stricker, S., Becker, J., Rupps, R., Pantzar, T., Miertus, J., Botta, G., Naretto, V.G., Janetzki, C., Yaqoob, N., Ott, C.E., Seelow, D., Wieczorek, D., Fiebig, B., Wirth, B., Hoopmann, M., Walther, M., Korber, F., Blankenburg, M., Mundlos, S., Heller, R. and Hoffmann, K. 2008, Am. J. Hum. Genet., 82, 464.
28. Ohno, K., Engel, A.G., Brengman, J.M., Shen, X.-M., Heidenrich, F.R., Vincent, A., Milone, M., Tan, E., Demirci, M., Walsh, P., Nakano, S. and Akiguchi, I. 2000, Ann. Neurol., 47, 162.
29. Croxen, R., Hatton, C., Shelley, C., Brydson, M., Chauplannaz, G., Oosterhuis, H., Vincent, A., Newsom-Davis, J., Colquhoun, D. and Beeson, D. 2002, Neurology, 59, 162.
30. Croxen, R., Newland, C., Beeson, D., Oosterhuis, H., Chauplannaz, G., Vincent, A. and Newsom-Davis, J. 1997, Hum. Mol. Genet., 6, 767.
31. Engel, A.G., Ohno, K., Milone, M., Wang, H.L., Nakano, S., Bouzat, C., Pruitt, J.N., 2nd, Hutchinson, D.O., Brengman, J.M., Bren, N., Sieb, J.P. and Sine, S.M. 1996, Hum. Mol. Genet., 5, 1217.
32. Wang, H.-L., Auerbach, A., Bren, N., Ohno, K., Engel, A.G. and Sine, S.M. 1997, J. Gen. Physiol., 109, 757.
33. Vohra, B.P., Groshong, J.S., Maselli, R.A., Verity, M.A., Wollmann, R.L. and Gomez, C.M. 2004, Ann. Neurol., 55, 347.
34. Ohno, K., Wang, H.-L., Shen, X.-M., Milone, M., Brengman, J.M., Bernasconi, L., Sine, S.M. and Engel, A.G. 2000, Neurology, 54 (Suppl 3), A183 (abstract).
35. Abdelgany, A., Wood, M. and Beeson, D. 2003, Hum. Mol. Genet., 12, 2637.
36. Milone, M., Wang, H.L., Ohno, K., Fukudome, T., Pruitt, J.N., Bren, N., Sine, S.M. and Engel, A.G. 1997, J. Neurosci., 17, 5651.
37. Shen, X.M., Deymeer, F., Sine, S.M. and Engel, A.G. 2006, Ann. Neurol., 60, 128.
38. Gomez, C.M., Maselli, R., Staub, J., Day, J.W., Cens, T., Wollmann, R.L. and Charnet, P.C. 1998, Soc Neurosci Abstr, 24, 484 (abstract).
39. Gomez, C.M., Maselli, R., Gammack, J., Lasalde, J., Tamamizu, S., Cornblath, D.R., Lehar, M., Mcnamee, H. and Kuncl, R.W. 1996, Ann. Neurol., 39, 712.
40. Shen, X.M., Ohno, K., Milone, M., Brengman, J.M., Tsujino, A. and Engel, A.G. 2003, Mol. Biol. Cell, 14 (Suppl), 223a (abstract).
41. Gomez, C.M., Maselli, R.A., Vohra, B.P., Navedo, M., Stiles, J.R., Charnet, P., Schott, K., Rojas, L., Keesey, J., Verity, A., Wollmann, R.W. and Lasalde-Dominicci, J. 2002, Ann. Neurol., 51, 102.
42. Shelley, C. and Colquhoun, D. 2005, J Physiol, 564, 377.
43. Hatton, C.J., Shelley, C., Brydson, M., Beeson, D. and Colquhoun, D. 2003, J Physiol, 547, 729.
44. Shen, X.M., Ohno, K., Fukudome, T., Tsujino, A., Brengman, J.M., Engel, A.G., DeVivo, D.C. and Packer, R.J. 2002, J. Neurol. Sci., 199 (Suppl 1), S96 (abstract).
45. Fidzianska, A., Ryniewicz, B., Shen, X.M. and Engel, A.G. 2005, Neuromuscul. Disord., 15, 753.
46. Outteryck, O., Richard, P., Lacour, A., Fournier, E., Zephir, H., Gaudon, K., Eymard, B., Hantai, D., Vermersch, P. and Stojkovic, T. 2009, J. Neurol. Neurosurg. Psychiatry, 80, 450.
47. Ohno, K., Milone, M., Brengman, J.M., LoMonaco, M., Evoli, A., Tonali, P.A. and Engel, A.G. 1998, Neurology, 50 (Suppl. 4), A432 (abstract).
48. Gomez, C.M. and Gammack, J.T. 1995, Neurology, 45, 982.
49. Shen, X.-M., Ohno, K., Tsujino, A., Brengman, J.M., Gingold, M., Sine, S.M. and Engel, A.G. 2003, J. Clin. Invest., 111, 497.

50. Webster, R., Brydson, M., Croxen, R., Newsom-Davis, J., Vincent, A. and Beeson, D. 2004, Neurology, 62, 1090.
51. Wang, H.-L., Milone, M., Ohno, K., Shen, X.-M., Tsujino, A., Batocchi, A.P., Tonali, P., Brengman, J., Engel, A.G. and Sine, S.M. 1999, Nat. Neurosci., 2, 226.
52. Shen, X.M., Fukuda, T., Ohno, K., Sine, S.M. and Engel, A.G. 2008, J. Clin. Invest., 118, 1867.
53. Brownlow, S., Webster, R., Croxen, R., Brydson, M., Neville, B., Lin, J.P., Vincent, A., Newsom-Davis, J. and Beeson, D. 2001, J. Clin. Invest., 108, 125.
54. Ohno, K., Wang, H.-L., Milone, M., Bren, N., Brengman, J.M., Nakano, S., Quiram, P., Pruitt, J.N., Sine, S.M. and Engel, A.G. 1996, Neuron, 17, 157.
55. Shen, X.-M., Ohno, K., Milone, M., Brengman, J.M., R., S.P. and Engel, A.G. 2001, Neurology, 56 (Suppl 3), A60 (abstract).
56. Sine, S.M., Shen, X.-M., Wang, H.-L., Ohno, K., Lee, W.-Y., Tsujino, A., Brengmann, J., Bren, N., Vajsar, J. and Engel, A.G. 2002, J. Gen. Physiol., 120, 483.
57. Milone, M., Wang, H.-L., Ohno, K., Prince, R., Fukudome, T., Shen, X.-M., Brengman, J.M., Griggs, R.C., Sine, S.M. and Engel, A.G. 1998, Neuron, 20, 575.
58. Wang, H.-L., Ohno, K., Milone, M., Brengman, J.M., Evoli, A., Batocchi, A.P., Middleton, L.T., Christodoulou, K., Engel, A.G. and Sine, S.M. 2000, J. Gen. Physiol., 116, 449.
59. Shen, X.-M., Ohno, K., Sine, S.M. and Engel, A.G. 2005, Brain, 128, 345.
60. Abicht, A., Stucka, R., Song, I.-H., Karcagi, V., Kugler, K., Baumgarten-Walczak, A., Stier, C., Pongratz, D., Mortier, W., Müller-Felber, W., Rüdel, R. and Lochmüller, H. 2000, Acta Myologica, 19, 23.
61. Groshong, J.S., Spencer, M.J., Bhattacharyya, B.J., Kudryashova, E., Vohra, B.P., Zayas, R., Wollmann, R.L., Miller, R.J. and Gomez, C.M. 2007, J. Clin. Invest., 117, 2903.
62. Fucile, S., Sucapane, A., Grassi, F., Eusebi, F. and Engel, A.G. 2006, J Physiol, 573, 35.
63. Di Castro, A., Martinello, K., Grassi, F., Eusebi, F. and Engel, A.G. 2007, J Physiol, 579, 671.
64. Fukudome, T., Ohno, K., Brengman, J.M. and Engel, A.G. 1998, Neuroreport, 9, 1907.
65. Harper, C.M. and Engel, A.G. 1998, Ann. Neurol., 43, 480.
66. Harper, C.M., Fukodome, T. and Engel, A.G. 2003, Neurology, 60, 1710.
67. Wirtz, P.W., Titulaer, M.J., Gerven, J.M. and Verschuuren, J.J. 2010, Expert Rev Clin Immunol, 6, 867.
68. Hesselmans, L.F., Jennekens, F.G., Van den Oord, C.J., Veldman, H. and Vincent, A. 1993, Anat. Rec., 236, 553.
69. Morgan, N.V., Brueton, L.A., Cox, P., Greally, M.T., Tolmie, J., Pasha, S., Aligianis, I.A., van Bokhoven, H., Marton, T., Al-Gazali, L., Morton, J.E., Oley, C., Johnson, C.A., Trembath, R.C., Brunner, H.G. and Maher, E.R. 2006, Am. J. Hum. Genet., 79, 390.
70. Hoffmann, K., Muller, J.S., Stricker, S., Megarbane, A., Rajab, A., Lindner, T.H., Cohen, M., Chouery, E., Adaimy, L., Ghanem, I., Delague, V., Boltshauser, E., Talim, B., Horvath, R., Robinson, P.N., Lochmuller, H., Hubner, C. and Mundlos, S. 2006, Am. J. Hum. Genet., 79, 303.
71. Giraud, M., Taubert, R., Vandiedonck, C., Ke, X., Levi-Strauss, M., Pagani, F., Baralle, F.E., Eymard, B., Tranchant, C., Gajdos, P., Vincent, A., Willcox, N., Beeson, D., Kyewski, B. and Garchon, H.J. 2007, Nature, 448, 934.

Protein-anchoring Strategy for Delivering Acetylcholinesterase to the Neuromuscular Junction

Mikako Ito[1], Yumi Suzuki[1], Takashi Okada[2], Takayasu Fukudome[3], Toshiro Yoshimura[4], Akio Masuda[1], Shin'ichi Takeda[2], Eric Krejci[5] and Kinji Ohno[1]

[1]*Division of Neurogenetics, Center for Neurological Diseases and Cancer, Nagoya University Graduate School of Medicine, Nagoya, Japan;* [2]*Department of Molecular Therapy, National Institute of Neuroscience, National Center of Neurology and Psychiatry, Tokyo, Japan;* [3]*Division of Clinical Research, Nagasaki Kawatana Medical Center, Nagasaki, Japan;* [4]*Department of Occupational Therapy, Nagasaki University School of Health Sciences, Nagasaki, Japan;* [5]*Université Paris Descartes, CNRS, UMR8194 , Paris, France*

Acetylcholinesterase (AChE) at the neuromuscular junction (NMJ) is anchored to the synaptic basal lamina *via* a triple helical collagen Q (ColQ). Congenital defects of ColQ cause endplate AChE deficiency and myasthenic syndrome. A single intravenous administration of adeno-associated virus serotype 8 (AAV8)-*COLQ* to *Colq*$^{-/-}$ mice recovered motor functions, synaptic transmission, as well as the morphology of the NMJ. ColQ-tailed AChE was specifically anchored to NMJ and its amount was restored to 89% of the wild type. We next characterized the molecular basis of this efficient recovery. We first confirmed that ColQ-tailed AChE can be specifically targeted to NMJ by an *in vitro* overlay assay in *Colq*$^{-/-}$ mice muscle sections. We then injected AAV1-*COLQ-IRES-EGFP* into the left tibialis anterior and detected AChE in noninjected limbs. Furthermore, the *in vivo* injection of recombinant ColQ-tailed AChE protein complex into the gluteus maximus muscle of *Colq*$^{-/-}$ mice led to accumulation of AChE in noninjected forelimbs. We demonstrated for the first time *in vivo* that the ColQ protein contains a tissue-targeting signal that is sufficient for anchoring itself to the NMJ. We propose that the protein-anchoring strategy is potentially applicable to a broad spectrum of diseases affecting extracellular matrix molecules.

Received 28 September 2011; accepted 31 January 2012; advance online publication 28 February 2012. doi:10.1038/mt.2012.34

INTRODUCTION

Acetylcholine (ACh) released from the nerve terminal is rapidly hydrolyzed by acetylcholinesterase (AChE) at the vertebrate neuromuscular junction (NMJ) to terminate cholinergic transmission. Three tetramers of catalytic AChE subunits are linked by a triple helical collagen Q (ColQ) to constitute a ColQ-tailed AChE.[1] The ColQ-tailed AChE is assembled in the endoplasmic reticulum and the Golgi apparatus.[2,3] ColQ carries three domains: (i) an N-terminal proline-rich attachment domain that organizes the catalytic AChE subunits into a tetramer, (ii) a collagenic domain that forms a triple helix, and (iii) a C-terminal domain enriched in charged residues and cysteines. ColQ-tailed AChE is organized in a secretory pathway, excreted, and anchored into the synaptic basal lamina using two domains of ColQ (**Figure 1**). First, the collagen domain harbors two heparan sulfate proteoglycan (HSPG)-binding domains[4] that bind to heparan sulfate proteoglycan such as perlecan in the synaptic basal lamina.[5] Second, the C-terminal domain of ColQ binds to MuSK, a muscle-specific receptor tyrosine kinase, on the postsynaptic membrane.[6] Human congenital defects of ColQ cause endplate AChE deficiency, in which the neuromuscular transmission is compromised.[7–9] Endplate AChE deficiency is an autosomal recessive disorder, which manifests as generalized muscle weakness, fatigue, amyotrophy, scoliosis, and minor facial abnormalities. Thirty-nine mutations of *COLQ* are currently registered in the Human Gene Mutation Database at http://www.hgmd.cf.ac.uk/. Ephedrine is effective for myasthenic symptoms to some extent,[10,11] though the underlying mechanisms of ephedrine efficacy remain elusive. We have developed a mouse model deficient in ColQ by deletion of the PRAD domain.[12] This strain recapitulates the phenotype of congenital myasthenic syndromes with AChE deficiency.

Gene therapy of endplate AChE deficiency is a complex issue both in humans and mice because ColQ is encoded by alternative promoters with a specific expression in subsynaptic nuclei of slow- and fast-twitch muscles.[13] The levels of AChE at the NMJ are supposed to be precisely controlled by the expression of ColQ and AChE,[14] as well as by a post-translational mechanism.[3] To treat endplate AChE deficiency in *Colq*-deficient mice, we delivered *COLQ* using adeno-associated virus (AAV) serotype 8, which has a tropism for muscles.[15] We used human *COLQ* instead of mouse *Colq* to foresee if the recombinant human *COLQ* is applicable to clinical practice in the future. Efficient rescue of AChE at the NMJ of AAV8-*COLQ*-injected mice prompted us to search for the molecular basis of these unexpected effects. We found that ColQ carries tissue-targeting signals that are necessary and sufficient to cluster AChE at the NMJ. This is the first report of a long-distance delivery of a large extracellular matrix complex over 50 nm in length and weighing over one million kDa in skeletal muscle. The findings of

Correspondence: *Kinji Ohno, Division of Neurogenetics, Center for Neurological Diseases and Cancer, Nagoya University Graduate School of Medicine, 65 Tsurumai, Showa-ku, Nagoya 466-8550, Japan, E-mail: ohnok@med.nagoya-u.ac.jp*

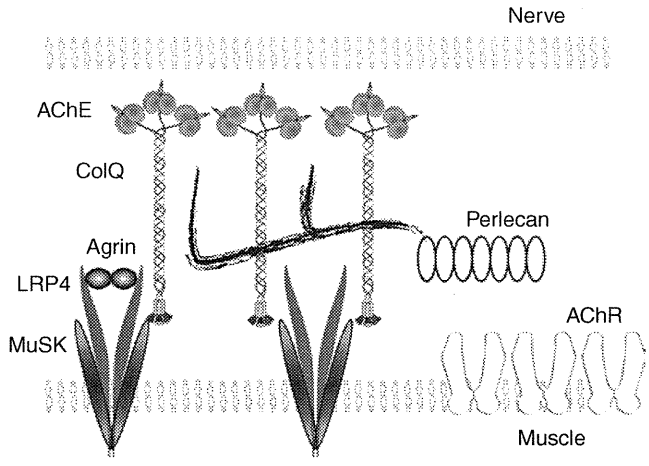

Figure 1 Schematic of anchoring of collagen Q (ColQ) to neuromuscular junction (NMJ). Twelve catalytic subunits of acetylcholinesterase (AChE) are attached to ColQ to form ColQ-tailed AChE. Two heparan sulfate proteoglycan-binding domains of ColQ are bound to perlecan. C-terminal domain of ColQ is bound to muscle-specific kinase (MuSK). Nerve-derived agrin binds to an LRP4–MuSK complex and induces rapsyn-mediated clustering of acetylcholine receptors (AChR) by phosphorylating AChR.

the present study open a new therapeutic avenue for treating many inherited defects of extracellular matrix proteins.

RESULTS

Intravenous administration of AAV8-*COLQ* normalizes motor functions of *Colq*$^{-/-}$ mice

We explored the recovery of the muscular phenotype of *Colq*$^{-/-}$ mice by viral delivery of a functional ColQ molecule. Therefore, we constructed a recombinant AAV serotype 8 carrying human *COLQ* cDNA. AAV serotype 8 (AAV8) is efficiently delivered to skeletal muscle after systemic injection.[16] We intravenously administered 1×10^{11}–2×10^{12} viral genome (vg) copies of AAV8-*COLQ* into 4-week-old *Colq*$^{-/-}$ mice. These mice exhibit muscle weakness, myasthenia, tremor, kyphosis, involuntary vocalization, and a slower growth rate than their wild-type littermates.[12] However, a single injection of 2×10^{12} vg, gradually improved their motor function to reach the level of that of wild type (**Figure 2a**). Furthermore, there were no signs of fatigue 6 weeks after the therapeutical injection (**Figure 2b**). Voluntary exercise in the treated mice also increased gradually but did not reach the level of wild type even at 5 weeks after injection (**Figure 2c**). The improved motor activities of treated mice are also demonstrated in **Supplementary Video 1**. Pairs of treated mice gave birth to *Colq*$^{-/-}$ pups and reared them to maturity. In longitudinal studies of three treated mice, all survived 18–20 months. Motor functions of the treated mice were declined at 48 weeks after injection but to the similar levels as those of wild type (**Figure 2a,c**). These observations clearly indicate the long-term therapeutic potential of a single viral injection of AAV.

AAV8-*COLQ* normalizes the neuromuscular synaptic transmission

To estimate recovery of neuromuscular transmission, we performed electrophysiological studies (**Table 1**). Treatment with

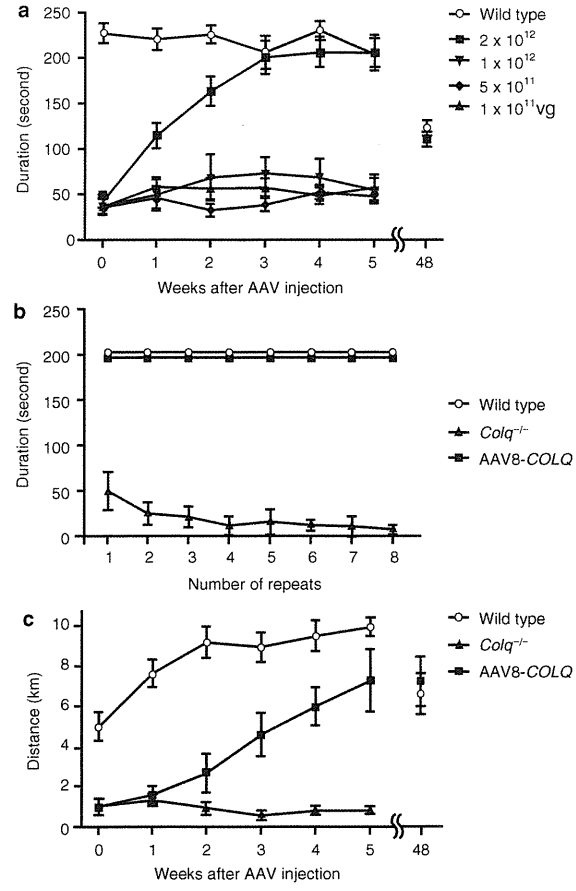

Figure 2 Exploration of motor function after intravenous injection of AAV8-*ColQ* to the tail vein of *Colq*$^{-/-}$ mice. (**a**) Motor function on the rotarod. The rotation was linearly accelerated from 0 to 40 r.p.m. in 240 seconds. Five groups of six mice were studied. Each group consisted of 4-week old mice and was either injected or not (control group) with increasing numbers of viral particles. Three weeks after their AAV8-*COLQ* injection, only the group of mice treated with 2×10^{12} vg remained on the rod as long as the wild-type littermates. Importantly, there was a progressive motor function recovery during the first 3 weeks after injection of *Colq*$^{-/-}$ mice. Symbols indicate mean and SE of six mice for each experiment. Mean and SE of the durations on the rotarod of two treated mice at 48 weeks after treatment is indicated along with that of the four age-matched wild-type mice. (**b**) Fatigue test using the rotarod was performed on three groups of a total of 18 mice. The rotation speed was fixed at 10 r.p.m. and the mice were immediately placed back on the rod each time they fell. Mice injected with 2×10^{12} vg exhibited no fatigue at 6 weeks after injection, whereas untreated *Colq*$^{-/-}$ mice fell increasingly more rapidly off the rod. (**c**) Voluntary movements were quantified by a counter-equipped running wheel. Plots show mean and SE of the number of rotations over 24 hours in each group of six mice (wild type, *Colq*$^{-/-}$, and AAV8-*COLQ*). Only the group of mice treated with 2×10^{12} vg increased the number of rotations every week but they did not reach the level of wild-type mice at 5 weeks after injection. Mean and SE of the number of rotations of two treated mice at 48 weeks after treatment is indicated along with that of the four age-matched wild-type mice. AAV8, adeno-associated virus serotype 8; ColQ, collagen Q.

AAV8-*COLQ* reduced decrements of the compound muscle action potentials in response to repetitive nerve stimulation at 2 Hz, reduced the amplitudes of miniature endplate potentials (MEPPs), shortened the miniature endplate potential decay time constants (**Figure 3**), and acquired responses to neostigmine. Endplate potential quantal content, which was decreased in

Table 1 Repetitive nerve stimulation and microelectrode studies

	Wild type	Wild type with neostigmine	*Colq*$^{-/-}$	*Colq*$^{-/-}$ with neostigmine	Treated *Colq*$^{-/-}$	Treated *Colq*$^{-/-}$ with neostigmine
Repetitive nerve stimulation[a]	0.92 ± 0.01* (2)	n.a.	0.58 ± 0.05 (3)	n.a.	0.76 ± 0.02* (3)	n.a.
EPP quantal content[b]	39.8 ± 2.3** (18)	n.a.	28.2 ± 1.8 (19)	n.a.	24.1 ± 1.6 (18)	n.a.
MEPP amplitude (mV)[c]	0.77 ± 0.04** (31)	1.52 ± 0.12 (18)	1.52 ± 0.11 (19)	1.52 ± 0.07 (10)	0.68 ± 0.02** (25)	0.98 ± 0.05** (24)
EPP amplitude (mV)[d]	30.6	n.a.	42.9	n.a.	16.4	n.a.
MEPP decay time (ms)[c]	1.77 ± 0.06** (31)	2.27 ± 0.08** (18)	3.07 ± 0.12 (19)	2.99 ± 0.09 (10)	2.45 ± 0.08** (25)	3.66 ± 0.09** (24)

Abbreviations: AChR, acetylcholine receptors; ColQ, collagen Q; EPP, endplate potential; MEPP, miniature endplate potential; n.a., not applicable.
Values represent mean ± SE. T = 29 ± 0.5 °C for EPP and MEPP recordings. Numbers in parenthesis indicate the number of recordings for repetitive nerve stimulation and the number of EPs from one or two mice for the other assays.
[a]Repetitive nerve stimulations were performed at 2 Hz, and the relative areas of compound muscle action potential (CMAP) of the fourth to the first stimulations are indicated. [b]Quantal content of EPP at 0.5 Hz stimulation corrected for resting membrane potential of –80 mV, nonlinear summation, and non-Poisson release. As the quantal contents of EPP are higher than 10, corrected values are indicated according to Cull-Candy *et al.*[45c] Normalized for resting membrane potential of –80 mV and a mean muscle fiber diameter of 55 µm. The actual fiber diameters were 45 ± 3.6 µm (mean ± SD, n = 31) for wild-type mice, 43 ± 3.0 µm (n = 19) for *Colq*$^{-/-}$ mice, and 46 ± 4.2 µm (n = 25) for the treated *Colq*$^{-/-}$ mice. [d]Estimated EPP amplitude is the product of the EPP quantal content and the MEPP amplitude. As AChR was partly blocked with curare for EPP recordings and not for MEPP recordings, we could not directly measure EPP amplitudes. Predicted low EPP amplitudes in treated mice suggest that the improvement of motor function was likely due to amelioration of depolarization block and/or of endplate myopathy.
*P < 0.05 and **P < 0.001 compared to *Colq*$^{-/-}$ mice by Student's t-test.

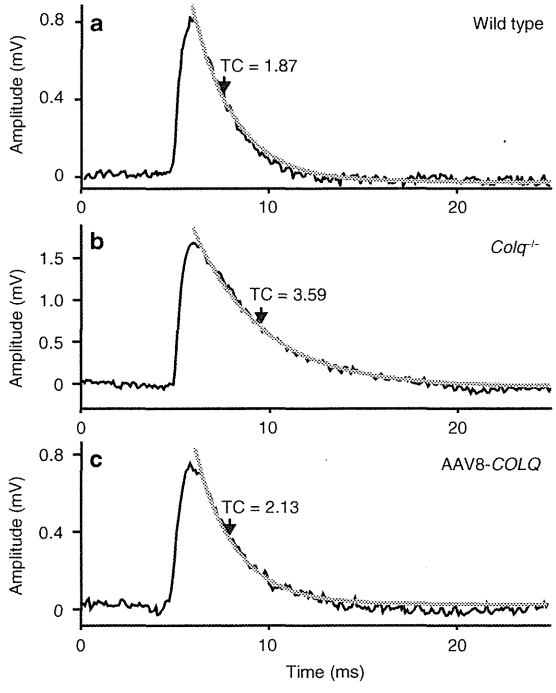

Figure 3 Representative miniature endplate potential (MEPP) recordings of diaphragm muscles of (a) wild type, (b) *Colq*$^{-/-}$, and (c) AAV8-*COLQ*-treated mice. (**b**) *Colq*$^{-/-}$ mice have higher MEPP amplitude and a longer decay time constant (TC) than (**a**) wild-type mice. AAV8-*COLQ* treatment shortened the decay TC and lowered the MEPP amplitude. Gray lines represent fitted exponential decay curves. AAV8, adeno-associated virus serotype 8; ColQ, collagen Q.

Colq$^{-/-}$ mice, was further decreased by the treatment, in contrast to our expectation.

Human ColQ-tailed AChE is anchored to the mouse NMJ *in vivo*

To further evaluate that the rescue was due to restitution of AChE at the NMJ, we used histological methods to visualize ColQ and AChE on muscle sections (**Figure 4a–c**). ColQ and AChE were colocalized to acetylcholine receptors (AChR) at the NMJ, confirming that ColQ-tailed AChE was specifically clustered to the target tissue. Although, we failed to observe improvement of motor functions with 1 × 10^{12} vg or less (**Figure 2a**), we still detected ColQ and AChE at NMJs with smaller amounts (data not shown). This suggests that a certain amount of viral genomes is required to exhibit improvement of motor deficits.

The ultrastructural morphology of treated mice also improved compared with age-matched *Colq*$^{-/-}$ mice (**Figure 4d–f**). The NMJ ultrastructures were variable from one to another in wild type, *Colq*$^{-/-}$, and treated mice, and we quantified the electron micrograph pictures (**Supplementary Table S1**). Quantitative analysis of presynaptic ultrastructures demonstrated that, in soleus slow-twitch muscle, Schwann cell invagination was mitigated, which increased the nerve terminal length, but the nerve terminal area remained essentially the same. Postsynaptic area and postsynaptic membrane length were also increased in soleus muscle of treated mice. In the extensor digitorum longus fast-twitch muscle, however, significant improvement was observed only in the ratio of enwrapped nerve terminal. Thus, the morphological improvements were more prominent in the soleus rather than in extensor digitorum longus muscles.

AAV8-*COLQ* restores the amount of ColQ-tailed AChE in the muscle to 89.3% of wild type

To estimate the efficiency of intravenous administration of AAV8-*COLQ*, we quantified the amount of the transduced *COLQ* mRNA, as well as ColQ-tailed AChE, in the muscle. We estimated the amount of *COLQ* mRNA in hindlimbs by a TaqMan probe, and found that the treated mice expressed the transduced *COLQ* at 92.5 ± 47.8% (mean ± SE, n = 4) of wild type. ColQ-tailed AChE from hindlimbs of the treated mice was fractionated by sucrose density-gradient ultracentrifugation. Sedimentation analysis revealed that AAV8-*COLQ* muscles have similar peaks of ColQ-tailed AChE species as those of wild type (**Figure 5a–c**). We also quantified the amount of globular AChE and ColQ-tailed AChE in gastrocnemius muscles of treated mice (**Figure 5d**). As previously reported, the amount of globular AChE was slightly lower in *Colq*$^{-/-}$ mice,[12] and this was normalized by treatment

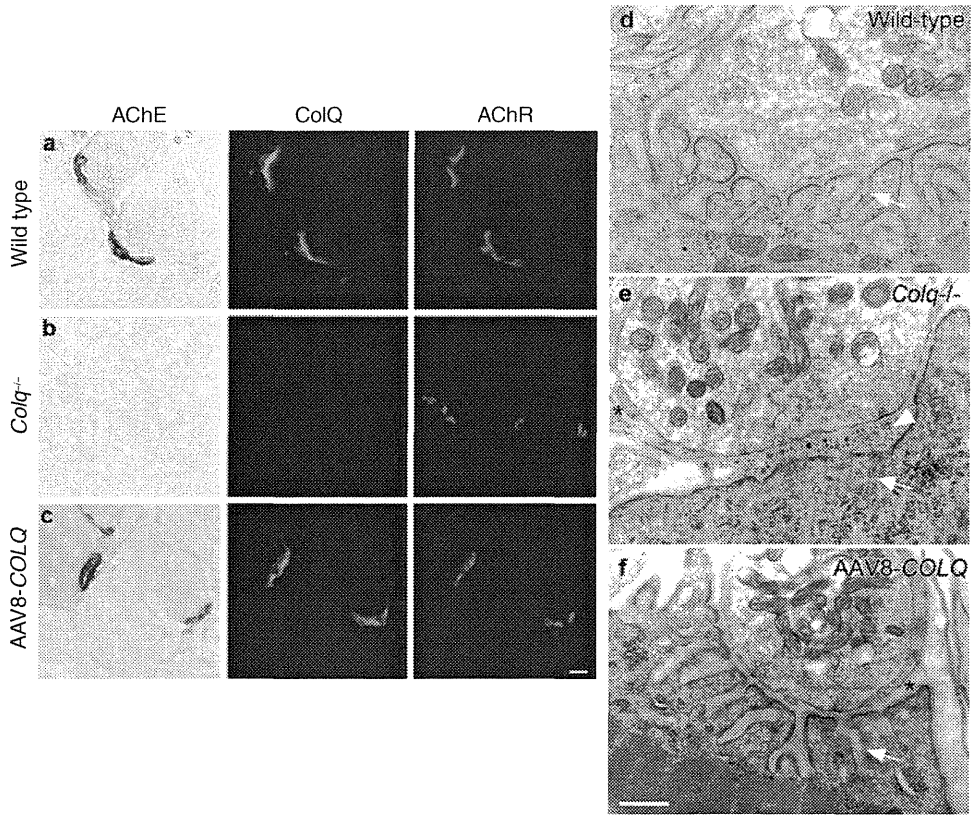

Figure 4 Histologies and ultrastructures of the neuromuscular junctions (NMJs). Localization of acetylcholinesterase (AChE) activity, collagen Q (ColQ), and acetylcholine receptors (AChR) in quadriceps muscles of (**a**) wild type, (**b**) *Colq*$^{-/-}$, and (**c**) AAV8-*COLQ* mice. Mice treated with 2 × 10^{12} vg of intravenous AAV8-*COLQ* express ColQ-tailed AChE at NMJ. AChE is stained for its activity. ColQ and AChR are detected by the polyclonal anti-ColQ antibody and α-bungarotoxin, respectively. Bar = 10 μm (**a–c**). Representative stainings of six mice in each group are indicated. Ultrastructures of soleus muscle NMJ (**d–f**). (**e**) *Colq*$^{-/-}$ mice show simplified synaptic clefts (arrow) and widening of the synaptic space (arrow head), whereas the NMJ ultrastructure of AAV8-*COLQ* mice (**f**) is indistinguishable from that of wild type (**d**). AAV8-*COLQ* mice still have small nerve terminals and invaginated Schwann cells (*). Bar = 1 μm (**d–f**). Representative ultrastructures of 27–41 electron micrograph (EM) pictures (see **Supplementary Table S1**) are indicated. AAV8, adeno-associated virus serotype 8.

with AAV8-*COLQ*. Treatment with AAV8-*COLQ* also restored ColQ-tailed AChE to 89.3 ± 9.6% (mean ± SD, $n = 4$) of wild type at 6 weeks after treatment. We also quantified ColQ-tailed AChE at 48 weeks after treatment and found that the amount was still 81.8 ± 21.6% (mean ± SD, $n = 2$) of the age-matched wild-type mice ($n = 3$). Although soleus slow-twitch muscle exhibited prominent improvement with the ultrastructural analysis, the available amount of soleus muscle was too small for the biochemical assay.

We also examined whether ColQ-tailed AChE was produced in the liver because AAV8 efficiently transduces hepatocytes.[15] AAV8-*COLQ* increased the *COLQ* mRNA level in the liver from 3.4 ± 0.34% (mean ± SE of five wild-type mice) to 61.3 ± 12.6% (mean ± SE of five treated mice) compared to those in the muscle of wild-type mice ($n = 5$). The *Ache* mRNA levels in the liver of wild type, *Colq*$^{-/-}$, and treated mice, however, were estimated to be <0.5% of that in wild-type muscle. The *Ache* mRNA levels in the liver were too low to be accurately quantified by real-time reverse transcription-PCR. Sedimentation profiles revealed no peaks of ColQ-tailed AChE in the liver of either wild type, *Colq*$^{-/-}$, or treated mice (**Supplementary Figure S1a–c**). This was probably due to lack of *Ache* expression. Globular AChE species observed in the sedimentation analysis was likely to represent AChE on the erythrocyte cell membrane.[17] These data suggest that AAV8-*COLQ* did not induce expression of ColQ-tailed AChE in the liver.

Local intramuscular injection of AAV8-*COLQ* expresses ColQ-tailed AChE at NMJs of noninjected limbs

Prominent improvements that we observed in AAV8-*COLQ*-treated mice raised a possibility that ColQ-tailed AChE moved from the transduced muscle cells to other muscle cells. We thus tested this possibility in the following experiments.

First, we have previously reported that the human recombinant ColQ-tailed AChE can be anchored to the synaptic basal lamina of the frog NMJ.[18] We tested this anchoring using mouse NMJs. We purified ColQ-tailed AChE expressed in HEK293 cells and incubated this with a section of skeletal muscle from *Colq*$^{-/-}$ mice. As expected, ColQ and AChE were detected at the mouse NMJ (**Supplementary Figure S2**), which supports the notion that ColQ-tailed AChE can be moved and anchored to the target *in vitro*.

Next, we tested whether ColQ-tailed AChE moved from the transduced muscles to the nontransduced muscles. We injected AAV8-*COLQ* to the left anterior tibial muscle. As expected, AChE and ColQ were rescued at the NMJs of the injected muscle. In addition, AChE and ColQ were also detected at all the examined

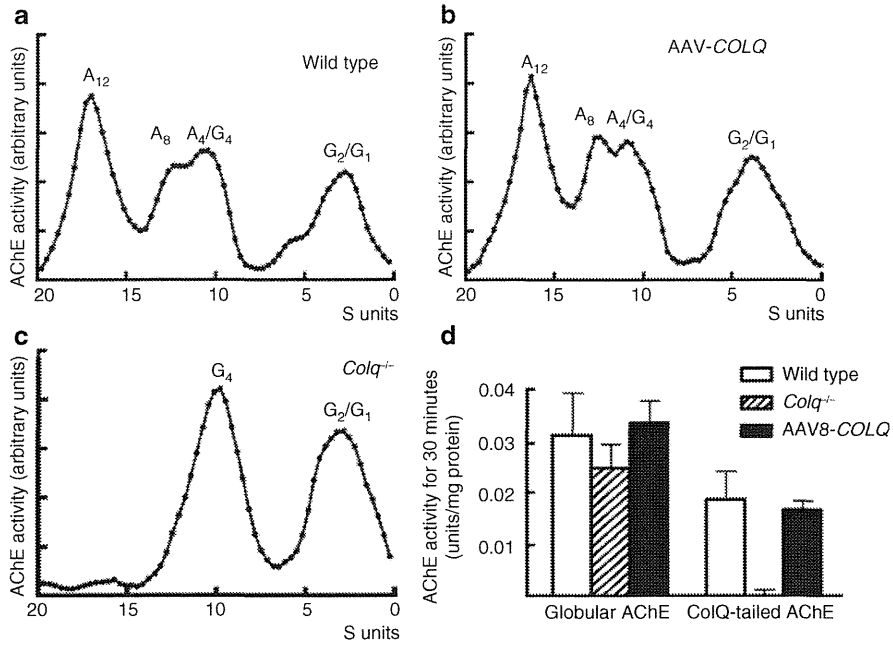

Figure 5 Quantification and biochemical analysis of acetylcholinesterase (AChE) recovery in muscles. Intravenous injection of 2×10^{12} vg of AAV8-*COLQ* into (**b**) *Colq*$^{-/-}$ mice gives rise to a sedimentation profile that is identical to that of (**a**) wild type, whereas (**c**) *Colq*$^{-/-}$ mice carry no collagen Q (ColQ)-tailed AChE. A_4, A_8, and A_{12} species carry 4, 8, and 12 AChE catalytic subunits attached to a triple helical ColQ. G_1, G_2, and G_4 species carry 1, 2, and 4 AChE catalytic subunits but without ColQ. A representative profile of three experiments is indicated. (**d**) Quantification of globular and ColQ-tailed AChE species (mean and SD, $n = 4$). The activity of ColQ-tailed AChE in the skeletal muscle of AAV8-*COLQ* mice is restored to 89 ± 10% of that of wild type. AAV8, adeno-associated virus serotype 8.

NMJs in noninjected muscles (data not shown). These results, however, could not exclude the possibility that AAV8-*COLQ* had been delivered to noninjected muscles in the form of a virus.

Local intramuscular injection of AAV1-*COLQ-IRES-EGFP* expresses ColQ-tailed AChE at NMJs of noninjected limbs

To reduce systemic delivery of AAV8 and to identify infected cells, we packed *COLQ* cDNA into the AAV serotype 1 (AAV1) that is known to transduce the injected muscle fibers locally.[19] In addition, we fused *COLQ* and internal ribosome entry site (*IRES*)-*EGFP* to express green fluorescent protein (GFP) in transduced cells synthesizing ColQ. We injected 2×10^{11} vg of AAV1-*COLQ-IRES-EGFP* into the left anterior tibial muscle of *Colq*$^{-/-}$ mice, while blocking the blood flow with a tourniquet for 20 minutes to restrict the distribution of the virus. The transduction efficiencies of AAV1-*COLQ-IRES-EGFP* were as follows: left anterior tibial muscle, 1.70 ± 0.29 viral copies per nucleus; right gastrocnemius muscle, 0.00100 ± 0.00079 copies; and bilateral brachial muscles, 0.00126 ± 0.00058 copies (mean ± SD, $n = 3$). Although only a fraction of the injected AAV1-*COLQ-IRES-EGFP* moved to noninjected limbs, we observed colocalization of ColQ and AChE at all the examined NMJs of right gastrocnemius, right tibialis anterior, both triceps, and both biceps in four examined mice (**Figure 6a**). We analyzed a total of 200–400 NMJs per muscle. In contrast, expression of intracellular enhanced GFP (EGFP) was not observed in noninjected limb muscles. We also quantified ColQ-tailed AChE in the noninjected bilateral forelimbs and right hindlimb, and found that the amounts were 21.5 ± 10.2% and 28.4 ± 10.0% (mean ± SD, $n = 4$), respectively, of those of wild type (**Figure 6b**).

ColQ-tailed AChE protein reaches and binds to remote NMJs

The presence of ColQ in noninjected muscles strongly suggests that the ColQ-tailed AChE is assembled intracellularly in one muscle and has moved to noninjected muscles, where it is anchored to the NMJs. To directly test this possibility, the gluteus maximus muscles of 5-week-old *Colq*$^{-/-}$ mice ($n = 4$) were injected daily with 2 μg of recombinant human ColQ-tailed AChE for 7 days. Histological analysis revealed the presence of ColQ and AChE in all of the examined NMJs from triceps muscles (**Figure 7a**). Quantitative analysis of ColQ signal intensities at the NMJs of noninjected triceps demonstrated that the ColQ-positive areas normalized for the AChR-positive area per NMJ became indistinguishable from that of wild type (**Figure 7b**). Furthermore, the ColQ signal intensity normalized for the AChR area per NMJs reached ~41.6% of that of wild type (**Figure 7c**). The *Colq*$^{-/-}$ mice could not hang on the wire at all, but the protein-injected mice acquired the ability to hang on the wire for two or more minutes from the fourth day of injection.

DISCUSSION

Effective and persistent gene therapy of ColQ with a single intravenous injection of AAV8-*COLQ*

We present an efficient and persistent recovery of AChE at the NMJ after a single intravenous administration of AAV8-*COLQ* in a *Colq*$^{-/-}$ mouse model of congenital myasthenic syndrome

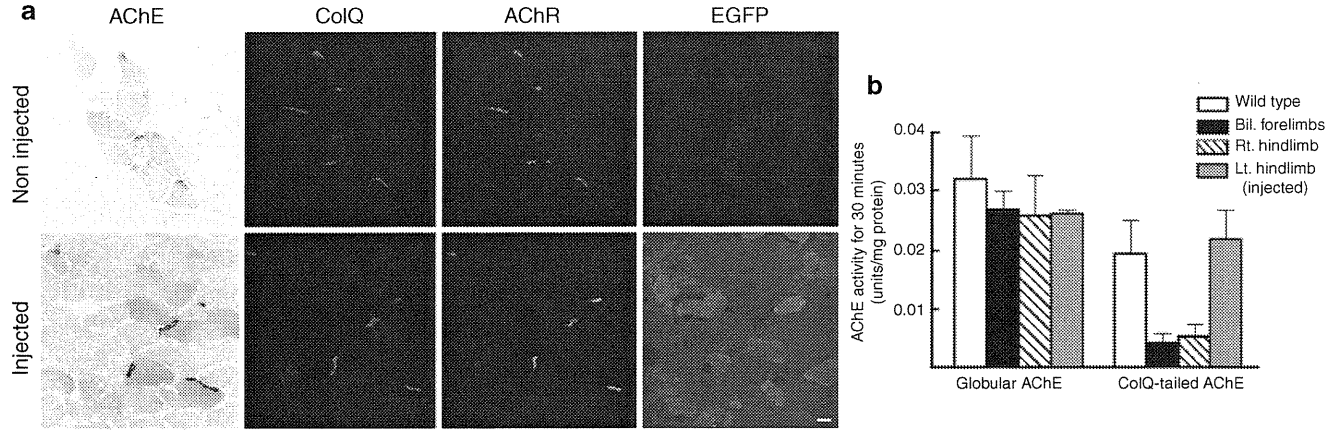

Figure 6 Intramuscular injection of 2×10^{11} vg of AAV1-*COLQ-IRES-EGFP* into the left anterior tibial muscle of *Colq*$^{-/-}$ mice. (**a**) Acetylcholinesterase (AChE) activity and collagen Q (ColQ) are colocalized to the acetylcholine receptors (AChR) in the injected muscle, as well as in the noninjected triceps muscle, although the signal intensities are not as high as those of the injected muscle. In contrast to ColQ, an intracellular molecule, enhanced green fluorescent protein (EGFP), is expressed only in the injected muscle, but not in the noninjected muscle. Bar = 10 μm. (**b**) Quantification of globular and ColQ-tailed AChE species of skeletal muscles (mean and SD, $n = 4$). In the injected left hindlimb, the activity of ColQ-tailed AChE is similar to that of wild type. In the noninjected both forelimbs and right hindlimb, the activities are 21.5 and 28.4% of wild type, respectively. AAV1, adeno-associated virus serotype 1.

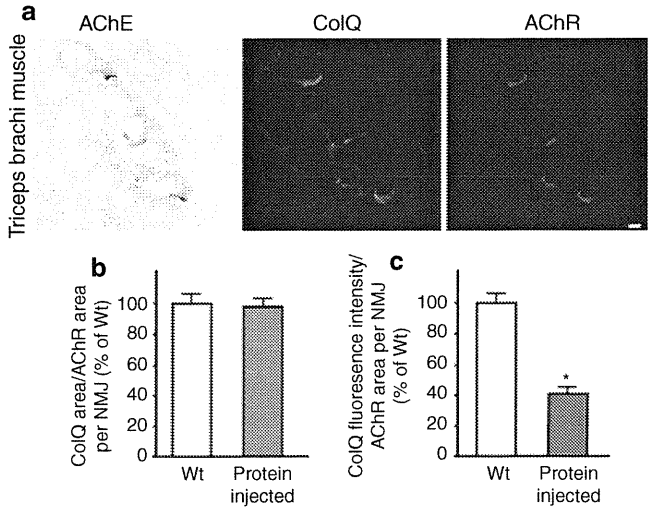

Figure 7 Injection of purified recombinant human collagen Q (ColQ)-tailed acetylcholinesterase (AChE). (**a**) Daily injection of 0.2 μg human recombinant ColQ-tailed AChE into the gluteus maximus muscles of *Colq*$^{-/-}$ mice rescues AChE activity and ColQ in the noninjected triceps where they are colocalized to acetylcholine receptors (AChR). Bar = 10 μm. (**b**) The size of ColQ-positive area is normalized for the size of AChR-positive area at the neuromuscular junctions (NMJs) of noninjected triceps. (**c**) Signal intensities of ColQ at the NMJs of noninjected triceps. Mean and SE are indicated. WT, wild-type mice, number of NMJs = 43; Protein injected, mice injected with ColQ-tailed AChE, number of NMJs = 42. *$P < 0.001$. Signal intensities are normalized to that of *Colq*$^{-/-}$ mice. Quantitative analyses were performed with the BZ-9000 microscope and the Dynamic Cell Count software BZ-H1C (Keyence).

with deficit in AChE. We observed ColQ-tailed AChE at all of the NMJs examined and the amount of the anchored AChE reached 89.3% of the wild-type level. The improved motor functions lasted at least 48 weeks after treatment and the treated mice survived 18–20 months, which is in contrast to at most 6-month lifespan of *Colq*$^{-/-}$ mice.[12] Although >99.5% of the vector genome stays episomal in mouse muscles even at 57 weeks after injection,[20,21] expression of the transgene in skeletal muscle lasts for 1.0–1.5 years without a decline in immunocompetent mice.[22,23] Our studies also underscore the long-lasting expression of the transgene delivered by AAV.

Rat *Colq*[24] and human *COLQ*[7] have two distinct promoters and generate ColQ1 and ColQ1a transcripts, which respectively include exon 1 and exon 1a and encode distinct signal peptides. A nerve-derived factor, calcitonin gene-related peptide, controls the expression of ColQ1a at the NMJs of fast-twitch muscles. However, in slow-twitch muscles, expression of ColQ1 occurs throughout the muscle fibers and is controlled by Ca^{2+}/calmodulin-dependent protein kinase II and myocyte enhancer factor 2.[24,25] As our viral construct was driven by the cytomegalovirus promoter, spatial and temporal regulation of ColQ expression should have been lost. In addition, our construct expressed ColQ1 and not ColQ1a, which was expected to be physiological for slow-twitch muscle but not for fast-twitch muscles. The prominent ultrastructural improvement in slow-twitch muscles rather than fast-twitch muscles may be partly because AAV8-*COLQ* encodes ColQ1 and not ColQ1a. This also suggests that the N-termini of ColQ1 and 1a have different functions. The pattern of ColQ expression resulting from our strategy was not physiological in three ways: (i) lack of subsynaptic nuclei-specific expression of ColQ, (ii) a ubiquitous cytomegalovirus promoter, and (iii) the exclusive expression of ColQ1. Despite these features, the motor and the synaptic functions are improved; AChE is locally accumulated at the NMJ in our treated mice. This suggests that the precise genetic control of the expression of ColQ is not the key factor for clustering of AChE and tissue-targeting signals of ColQ are sufficient to functionally restore AChE at the NMJ.

The protein-anchoring therapy

Although ColQ-tailed AChE in the serum of either wild type, *Colq*$^{-/-}$, or treated mice was less than a detection threshold in the

sedimentation analysis (**Supplementary Figure S1d–f**), anchoring of ColQ-tailed AChE to remote NMJs was supported by two lines of evidence: local intramuscular injections of AAV1-*COLQ-IRES-EGFP* (**Figure 6**) and of the purified recombinant ColQ-tailed AChE protein complex (**Figure 7**). In either case, AChE at the NMJ of the noninjected muscle originates from ColQ-tailed AChE arising from another source; not from local secretion and retention of ColQ-tailed AChE synthesized by subsynaptic nuclei followed by assembly and maturation in the postsynaptic area as in wild-type mice. The overlay of recombinant ColQ-tailed AChE *in vitro* either on normal muscle tissue sections of frog[5,18] or of *Colq*$^{-/-}$ mouse (**Supplementary Figure S2**) demonstrates that ColQ harbors a signal that targets AChE to the NMJ. The dual interactions of ColQ with MuSK[6] and perlecan,[5] which are both required in the overlay experiment,[18] are likely to restrict ColQ to the NMJ. In endplate AChE deficiency, point mutations that affect the binding of ColQ to MuSK prevent the accumulation of AChE.[18] Although no mutation has been reported at the heparan sulfate proteoglycan-binding domains of ColQ in endplate AChE deficiency, the reduction of perlecan mimicking Schwartz–Jampel syndrome reduces the level of AChE and ColQ at the NMJ.[26,27] All of these observations suggest that the combination of MuSK and perlecan determines the number of ColQ-tailed AChE anchored at the NMJ. This notion was previously termed as "molecular parking lots" by Rotundo and colleagues.[28]

ColQ-tailed AChE is a nanostructure made of a rigid collagen of 50-nm length and three AChE tetramers. ColQ-tailed AChE is apparently able to move from one muscle to another as demonstrated by clustering in the triceps muscle after protein injection into the gluteus. A similar approach is inherently employed by nature, as exemplified by fibronectin that is ubiquitously present in extracellular matrices and is largely derived from liver.[29] Injection of a protein complex is reported with laminin-111.[30] An intramuscularly or intraperitoneally injected laminin-111 is distributed to the basal lamina of skeletal and cardiac muscles in an mdx-mouse model of Duchenne muscular dystrophy. In contrast to our strategy, laminin-111 is not expressed or accumulated in normal or dystrophic adult muscles. Their studies exploit an ectopic deposition of laminin-111 to induce expression of α_7-integrin that stabilizes the sarcolemma of dystrophic muscle fibers.

The ColQ must be synthesized in cells that produce a splice variant T of AChE for obtaining the correct assembly of the complex.[2] A single muscle fiber harbors hundreds of nuclei that are functionally compartmentalized, and a molecule expressed in a single nucleus goes through the muscle fiber only for a short distance.[31,32] Thus, the multinucleation of muscle fibers is unlikely to have contributed to the restoration of function in the *Colq*$^{-/-}$ mice of our study. Similar specific clustering of a muscle-generated protein to the NMJ has been reported with laminin β2.[33] When laminin β2 is expressed throughout muscle fibers by the MCK promoter in transgenic mice, it is clustered at the NMJ.

The inability to achieve efficient and specific delivery of a transgene to the target tissue often prevents the application of gene therapy to model animals and patients.[34] Here, we propose the protein-anchoring strategy that provides a new therapeutic approach for congenital defects of extracellular matrix proteins.[35] The potential candidate molecules of the protein-anchoring therapy include laminin α2 causing laminin-α2-deficient congenital muscular dystrophy,[36] perlecan causing Schwartz–Jampel syndrome,[26,37] and collagen VI causing Ullrich syndrome.[38] It should be emphasized that this strategy can be potentially used for a huge number of diseases caused by mutations of genes encoding proteins of the extracellular matrices in general.

MATERIALS AND METHODS

Preparation of AAV carrying COLQ. Human *COLQ* cDNA[7] was cloned into pAAV-MCS (AAV Helper-Free system; Stratagene, Santa Clara, CA) that carries the cytomegalovirus promoter to obtain a pAAV-*COLQ*. We also inserted *IRES-EGFP* to make pAAV-*COLQ-IRES-EGFP*. To make AAV8-*COLQ*, HEK293 cells were cotransfected with the following plasmids: the proviral vector plasmid pAAV-*COLQ*, the AAV8 chimeric helper plasmid pRC8, and the adenoviral helper plasmid pHelper (Stratagene) using calcium phosphate coprecipitation method.[39] To make AAV1-*COLQ-IRES-EGFP*, we transfected HEK293 cells with pAAV-*COLQ-IRES-EGFP*, the AAV1 chimeric helper plasmid pRep2Cap1, and pHelper. The AAV particles were concentrated by CsCl gradient ultracentrifugation for 3 hours[40] and further purified with the quick dual ion-exchange procedures.[41] The viral titer was estimated by quantitative PCR in real-time using MX3000p (Stratagene).[42]

Administration of AAV carrying COLQ to Colq*$^{-/-}$ *mice. All animal studies were approved by the Animal Care and Use Committee of the Nagoya University Graduate School of Medicine. For intravenous administration, 1×10^{11}–2×10^{12} vg of AAV8-*COLQ* were injected into the tail vein of 4-week-old *Colq*$^{-/-}$ mice.[12] For intramuscular administration, 2×10^{11} vg of AAV1-*COLQ-IRES-EGFP* were injected into the left anterior tibial muscle of 4-week-old *Colq*$^{-/-}$ mice. The left proximal thigh was tightly ligated with a tourniquet for 20 minutes during intramuscular injection to prevent vascular delivery of viral particles throughout the body.

Motor activity tests. Muscle weakness and fatigability were measured with a rotarod apparatus (Ugo, Basile, Italy). Mice were first trained three times to be accommodated to the task. Mice were consecutively examined three times and were allowed to take a rest for 1 hour between individual tasks.

Running-wheel activity was used to quantify voluntary exercises. Each mouse was placed in a standard cage equipped with a counter-equipped running wheel (diameter, 14.7 cm, width, 5.2 cm; Ohara Medical, Tokyo, Japan). The running distances were recorded using the counter every 24 hours.

Histology. We raised a polyclonal ColQ antibody by injecting a synthetic peptide of SAALPSLDQKKRGGHKAC, corresponding to codons 34–51 in human ColQ, into rabbits. We confirmed that the raised antibody recognized ColQ by western blotting (**Supplementary Figure S3**) and that no signal was present in a section of *Colq*$^{-/-}$ mice (**Figure 4b** and **Supplementary Figure S2**). Mice were sacrificed at 6 weeks after treatment. Skeletal muscles of mice were frozen in the liquid nitrogen-cooled isopentane and sectioned at 8-μm thick with a Leica CW3050-4 cryostat at −20 °C. Muscle sections were blocked with 5% horse serum in phosphate-buffered saline for 20 minutes and incubated with the primary antibody (1:100) for 2 hours. Sections were then incubated with a secondary antibody (1:100) for 1 hour, along with Alexa-594-conjugated α-bungarotoxin (2.5 μg/ml) (Sigma, St Louis, MO) for visualizing AChR. Anti-rabbit and anti-mouse secondary antibodies were both FITC-labeled (Vector Lab, Burlingame, CA). For AAV1-*COLQ-IRES-EGFP*, we detected ColQ using anti-rabbit secondary antibody labeled with rhodamine (1:40; Santa Cruz, Santa Cruz, CA) and localized AChR by Alexa-647-conjugated α-bungarotoxin (2.5 μg/ml; Sigma). Signals of ColQ, AChE, AChR, and EGFP were examined with BX60 (Olympus, Tokyo, Japan) or BZ-9000 (Keyence, Osaka, Japan).

Mouse AChE activity was detected by the histochemical method at 6 weeks after treatment. Muscle sections were incubated for 20 minutes at 37 °C in the reaction mixture containing 1.73 mmol/l acetylthiocholine iodide, 38 mmol/l sodium acetate, 51 mmol/l acetic acid, 6 mmol/l sodium

citrate, 4.7 mmol/l copper sulfate, 0.5 mmol/l potassium ferricyanide, and 5×10^{-5} mol/l ethopropazine (Sigma), which is an inhibitor of butyrylcholinesterase.

Sedimentation biochemical analyses. Mice were sacrificed at 6 weeks after treatment. Sedimentation analysis was performed as previously described.[7] Proteins were extracted from the muscle and liver in a detergent buffer [10 mmol/l HEPES (pH 7.2), 1% CHAPS, 10 mmol/l EDTA, 2 mmol/l benzamidine, leupeptin (20 μg/ml) and pepstatin (10 μg/ml)] containing 0.8 mol/l NaCl. The eluate was applied on a 5–20% sucrose density gradient, which was made in the detergent buffer containing 0.8 mol/l NaCl, along with β-galactosidase (16S) and alkaline phosphatase (6.1S) as internal sedimentation standards. Centrifugation was performed in a Beckman SW41Ti rotor at 4°C for 21 hours at 38,000 r.p.m. AChE activity was assayed by the colorimetric method of Ellman in the presence of 5×10^{-5} mol/l ethopropazine.

For biochemical analysis, skeletal muscle was shattered by the Cool Mill (Toyobo, Osaka, Japan) in liquid nitrogen. We extracted globular forms of AChE into the NaCl-free detergent buffer, and ColQ-tailed AChE into detergent buffer containing 0.8 mol/l NaCl as previously described.[12] AChE activity was assayed using AChE-Specific Assay kit (Dojindo, Kumamoto, Japan) or the Ellman method and normalized by Torpedo AChE activity (Sigma).

Microelectrode studies. Phrenic nerve-diaphragm preparations were obtained from three wild type, three *Colq*$^{-/-}$, and three AAV8-*COLQ*-treated mice at 8 weeks of age, which corresponds to 4 weeks after treatment. We stimulated the sciatic nerve at 2 Hz and recorded compound muscle action potentials of gastrocnemius muscles using a needle electrode under deep anesthesia. For technical reasons, we could not analyze the limb muscles that we used in the other assays. After mice were sacrificed, miniature endplate potentials and evoked EPPs were recorded as described elsewhere.[43] Neostigmine methylsufate (Elkins-Sinn, Cherry Hill, NJ) was used at a concentration of 10^{-6} g/ml in the bath to block cholinesterases. We employed the AxoGraph × 1.1.6 (AxoGraph Scientific, Sydney, Australia) for data analysis.

Electron microscopy. For electron microscopy, extensor digitorum longus and soleus muscles were fixed in ice-cold 3% glutaraldehyde buffered with 0.1 mol/l cacodylate buffer (pH 7.3) at 4 weeks after treatment. The endplate-rich region of the muscle was refixed in 2% OsO_4 in cacodylate buffer, dehydrated, and embedded in Epon812.

All thin sections were cut transversely, stained with lead citrate, and photographed in a JEM 1,200 EX electron microscopy. Morphometric analysis of the motor endplate was performed following the procedure of Engel and Santa,[44] and included the following: (i) presynaptic membrane length, in μm; (ii) nerve terminal area, in μm^2; (iii) number of synaptic vesicles per unit area, in numbers per μm^2; (iv) length of processes of Schwann cells on presynaptic membrane, in μm; (v) percentage of totally enwrapped nerve terminal by processes of Schwann cells; (vi) postsynaptic area of folds and clefts associated with a given nerve terminal, in μm^2; (vii) postsynaptic membrane length associated with a given nerve terminal, in μm; (viii) postsynaptic membrane length per unit postsynaptic area (postsynaptic membrane density), derived by dividing the value of (vii) by that of (vi), in μm per μm^2; (ix) postsynaptic to presynaptic membrane ratio. Endplates were localized and analyzed by established methods, and peroxidase-labeled α-bungarotoxin was used for the ultrastructural localization of AChR.[45] The images were quantified using the NIH Image 1.62 software (National Institutes of Health).

Expression and purification of recombinant ColQ. The plasmids that previously introduced human *COLQ* and human *ACHE* cDNAs into a pTargeT (Promega, Madison, WI)[7] were cotransfected into HEK293 cells. Proteins were extracted from the cells in Tris–HCl buffer [50 mmol/l Tris–HCl (pH 7.0), 0.5% Triton X-100, 0.2 mmol/l EDTA, leupeptin (2 μg/ml), and pepstatin (1 μg/ml)] containing 1 mol/l NaCl. The extracts were loaded onto HiTrap Heparin HP columns (GE Healthcare, Buckinghamshire, UK). The concentration of purified recombinant ColQ-tailed AChE was equivalent to ~4 μg/ml Torpedo AChE. We injected 50 μl of the purified ColQ-tailed AChE in phosphate-buffered saline daily into the gluteus maximus muscles of 5-week-old *Colq*$^{-/-}$ mice for a week. Mice were given a single intraperitoneal injection of 300 mg/kg cyclophosphamide monohydrate (10 mg/ml in saline) at 24 hours after the first ColQ-tailed AChE injection to suppress immunoreaction against the recombinant human protein.[46] After 7 days, mice were sacrificed and brachial muscles were stained for ColQ molecule and AChE activity as described above.

Real-time PCR/reverse transcription-PCR. For expression analysis, total RNAs from skeletal muscle and liver cells were extracted using the RNeasy Mini kit (Qiagen, Hilden, Germany) with *DNase*I and proteinase K treatment according to the manufacturer's instructions. First-stranded cDNA was synthesized using the ReverTra Ace reverse transcriptase (Toyobo). Expressions of human *COLQ*, mouse *Colq*, and mouse *Ache* were analyzed using the TaqMan (Applied Biosystems, Foster city, CA) probes and primers in LightCycler 480 (Roche, Mannheim, Germany). We also quantified 18S rRNA for normalization.

To quantify the transduction efficiency, total DNA was extracted from skeletal muscle and liver using the QIAamp DNA Mini Kit (Qiagen). The amount of viral genome was quantified by real-time PCR using a TaqMan probe targeting to human *COLQ*, as well as to mouse *Tert* encoding telomerase reverse transcriptase to normalize for the cell numbers.

SUPPLEMENTARY MATERIAL

Figure S1. Sedimentation analyses of AChE in the liver and serum.
Figure S2. Binding of human ColQ-tailed AChE proteins to the NMJ in muscle section of *Colq*$^{-/-}$ mice.
Figure S3. Western blot of a newly raised rabbit polyclonal anti-ColQ antibody (1:1,000).
Table S1. Morphometric analysis of endplate ultrastructures.
Video 1. First part: Two *Colq*$^{-/-}$ mice treated with an intravenous administration of 2×10^{12} vg of AAV8-*COLQ* (right cage) move around actively.

ACKNOWLEDGMENTS

We thank James M. Wilson for providing the chimeric helper plasmid pRC8 (identical to p5E18-VD2/8) and pRep2Cap1 (identical to p5E18RXCI). This work was supported by Grants-in-Aid from the Ministry of Education, Culture, Sports, Science, and Technology of Japan, and the Ministry of Health, Labor, and Welfare of Japan, as well as by Grant from ANR maladies rares. The authors declared no conflict of interest.

REFERENCES

1. Krejci, E, Thomine, S, Boschetti, N, Legay, C, Sketelj, J and Massoulié, J (1997). The mammalian gene of acetylcholinesterase-associated collagen. *J Biol Chem* **272**: 22840–22847.
2. Rotundo, RL (1984). Asymmetric acetylcholinesterase is assembled in the Golgi apparatus. *Proc Natl Acad Sci USA* **81**: 479–483.
3. Ruiz, CA and Rotundo, RL (2009). Limiting role of protein disulfide isomerase in the expression of collagen-tailed acetylcholinesterase forms in muscle. *J Biol Chem* **284**: 31753–31763.
4. Deprez, P, Inestrosa, NC and Krejci, E (2003). Two different heparin-binding domains in the triple-helical domain of ColQ, the collagen tail subunit of synaptic acetylcholinesterase. *J Biol Chem* **278**: 23233–23242.
5. Peng, HB, Xie, H, Rossi, SG and Rotundo, RL (1999). Acetylcholinesterase clustering at the neuromuscular junction involves perlecan and dystroglycan. *J Cell Biol* **145**: 911–921.
6. Cartaud, A, Strochlic, L, Guerra, M, Blanchard, B, Lambergeon, M, Krejci, E *et al.* (2004). MuSK is required for anchoring acetylcholinesterase at the neuromuscular junction. *J Cell Biol* **165**: 505–515.
7. Ohno, K, Brengman, J, Tsujino, A and Engel, AG (1998). Human endplate acetylcholinesterase deficiency caused by mutations in the collagen-like tail subunit (ColQ) of the asymmetric enzyme. *Proc Natl Acad Sci USA* **95**: 9654–9659.
8. Donger, C, Krejci, E, Serradell, AP, Eymard, B, Bon, S, Nicole, S *et al.* (1998). Mutation in the human acetylcholinesterase-associated collagen gene, COLQ, is responsible

for congenital myasthenic syndrome with end-plate acetylcholinesterase deficiency (Type Ic). *Am J Hum Genet* **63**: 967–975.
9. Ohno, K, Engel, AG, Brengman, JM, Shen, XM, Heidenreich, F, Vincent, A *et al.* (2000). The spectrum of mutations causing end-plate acetylcholinesterase deficiency. *Ann Neurol* **47**: 162–170.
10. Bestue-Cardiel, M, Sáenz de Cabezón-Alvarez, A, Capablo-Liesa, JL, López-Pisón, J, Peña-Segura, JL, Martin-Martinez, J *et al.* (2005). Congenital endplate acetylcholinesterase deficiency responsive to ephedrine. *Neurology* **65**: 144–146.
11. Mihaylova, V, Müller, JS, Vilchez, JJ, Salih, MA, Kabiraj, MM, D'Amico, A *et al.* (2008). Clinical and molecular genetic findings in COLQ-mutant congenital myasthenic syndromes. *Brain* **131**(Pt 3): 747–759.
12. Feng, G, Krejci, E, Molgo, J, Cunningham, JM, Massoulié, J and Sanes, JR (1999). Genetic analysis of collagen Q: roles in acetylcholinesterase and butyrylcholinesterase assembly and in synaptic structure and function. *J Cell Biol* **144**: 1349–1360.
13. Lee, HH, Choi, RC, Ting, AK, Siow, NL, Jiang, JX, Massoulié, J *et al.* (2004). Transcriptional regulation of acetylcholinesterase-associated collagen ColQ: differential expression in fast and slow twitch muscle fibers is driven by distinct promoters. *J Biol Chem* **279**: 27098–27107.
14. Ruiz, CA and Rotundo, RL (2009). Dissociation of transcription, translation, and assembly of collagen-tailed acetylcholinesterase in skeletal muscle. *J Biol Chem* **284**: 21488–21495.
15. Inagaki, K, Fuess, S, Storm, TA, Gibson, GA, Mctiernan, CF, Kay, MA *et al.* (2006). Robust systemic transduction with AAV9 vectors in mice: efficient global cardiac gene transfer superior to that of AAV8. *Mol Ther* **14**: 45–53.
16. Nakai, H, Fuess, S, Storm, TA, Muramatsu, S, Nara, Y and Kay, MA (2005). Unrestricted hepatocyte transduction with adeno-associated virus serotype 8 vectors in mice. *J Virol* **79**: 214–224.
17. Bouma, SR, Drislane, FW and Huestis, WH (1977). Selective extraction of membrane-bound proteins by phospholipid vesicles. *J Biol Chem* **252**: 6759–6763.
18. Kimbell, LM, Ohno, K, Engel, AG and Rotundo, RL (2004). C-terminal and heparin-binding domains of collagenic tail subunit are both essential for anchoring acetylcholinesterase at the synapse. *J Biol Chem* **279**: 10997–11005.
19. Wang, Z, Zhu, T, Qiao, C, Zhou, L, Wang, B, Zhang, J *et al.* (2005). Adeno-associated virus serotype 8 efficiently delivers genes to muscle and heart. *Nat Biotechnol* **23**: 321–328.
20. Schnepp, BC, Clark, KR, Klemanski, DL, Pacak, CA and Johnson, PR (2003). Genetic fate of recombinant adeno-associated virus vector genomes in muscle. *J Virol* **77**: 3495–3504.
21. Kay, MA (2007). AAV vectors and tumorigenicity. *Nat Biotechnol* **25**: 1111–1113.
22. Xiao, X, Li, J and Samulski, RJ (1996). Efficient long-term gene transfer into muscle tissue of immunocompetent mice by adeno-associated virus vector. *J Virol* **70**: 8098–8108.
23. Rivière, C, Danos, O and Douar, AM (2006). Long-term expression and repeated administration of AAV type 1, 2 and 5 vectors in skeletal muscle of immunocompetent adult mice. *Gene Ther* **13**: 1300–1308.
24. Krejci, E, Legay, C, Thomine, S, Sketelj, J and Massoulié, J (1999). Differences in expression of acetylcholinesterase and collagen Q control the distribution and oligomerization of the collagen-tailed forms in fast and slow muscles. *J Neurosci* **19**: 10672–10679.
25. Lau, FT, Choi, RC, Xie, HQ, Leung, KW, Chen, VP, Zhu, JT *et al.* (2008). Myocyte enhancer factor 2 mediates acetylcholine-induced expression of acetylcholinesterase-associated collagen ColQ in cultured myotubes. *Mol Cell Neurosci* **39**: 429–438.
26. Arikawa-Hirasawa, E, Rossi, SG, Rotundo, RL and Yamada, Y (2002). Absence of acetylcholinesterase at the neuromuscular junctions of perlecan-null mice. *Nat Neurosci* **5**: 119–123.
27. Stum, M, Girard, E, Bangratz, M, Bernard, V, Herbin, M, Vignaud, A *et al.* (2008). Evidence of a dosage effect and a physiological endplate acetylcholinesterase deficiency in the first mouse models mimicking Schwartz-Jampel syndrome neuromyotonia. *Hum Mol Genet* **17**: 3166–3179.
28. Rotundo, RL, Rossi, SG and Anglister, L (1997). Transplantation of quail collagen-tailed acetylcholinesterase molecules onto the frog neuromuscular synapse. *J Cell Biol* **136**: 367–374.
29. Moretti, FA, Chauhan, AK, Iaconcig, A, Porro, F, Baralle, FE and Muro, AF (2007). A major fraction of fibronectin present in the extracellular matrix of tissues is plasma-derived. *J Biol Chem* **282**: 28057–28062.
30. Rooney, JE, Gurpur, PB and Burkin, DJ (2009). Laminin-111 protein therapy prevents muscle disease in the mdx mouse model for Duchenne muscular dystrophy. *Proc Natl Acad Sci USA* **106**: 7991–7996.
31. Hall, ZW and Ralston, E (1989). Nuclear domains in muscle cells. *Cell* **59**: 771–772.
32. Rossi, SG, Vazquez, AE and Rotundo, RL (2000). Local control of acetylcholinesterase gene expression in multinucleated skeletal muscle fibers: individual nuclei respond to signals from the overlying plasma membrane. *J Neurosci* **20**: 919–928.
33. Miner, JH, Go, G, Cunningham, J, Patton, BL and Jarad, G (2006). Transgenic isolation of skeletal muscle and kidney defects in laminin beta2 mutant mice: implications for Pierson syndrome. *Development* **133**: 967–975.
34. Somia, N and Verma, IM (2000). Gene therapy: trials and tribulations. *Nat Rev Genet* **1**: 91–99.
35. Mueller, C and Flotte, TR (2008). Clinical gene therapy using recombinant adeno-associated virus vectors. *Gene Ther* **15**: 858–863.
36. Helbling-Leclerc, A, Zhang, X, Topaloglu, H, Cruaud, C, Tesson, F, Weissenbach, J *et al.* (1995). Mutations in the laminin alpha 2-chain gene (LAMA2) cause merosin-deficient congenital muscular dystrophy. *Nat Genet* **11**: 216–218.
37. Nicole, S, Davoine, CS, Topaloglu, H, Cattolico, L, Barral, D, Beighton, P *et al.* (2000). Perlecan, the major proteoglycan of basement membranes, is altered in patients with Schwartz-Jampel syndrome (chondrodystrophic myotonia). *Nat Genet* **26**: 480–483.
38. Kawahara, G, Okada, M, Morone, N, Ibarra, CA, Nonaka, I, Noguchi, S *et al.* (2007). Reduced cell anchorage may cause sarcolemma-specific collagen VI deficiency in Ullrich disease. *Neurology* **69**: 1043–1049.
39. Okada, T, Nomoto, T, Yoshioka, T, Nonaka-Sarukawa, M, Ito, T, Ogura, T *et al.* (2005). Large-scale production of recombinant viruses by use of a large culture vessel with active gassing. *Hum Gene Ther* **16**: 1212–1218.
40. Okada, T, Shimazaki, K, Nomoto, T, Matsushita, T, Mizukami, H, Urabe, M *et al.* (2002). Adeno-associated viral vector-mediated gene therapy of ischemia-induced neuronal death. *Meth Enzymol* **346**: 378–393.
41. Okada, T, Nonaka-Sarukawa, M, Uchibori, R, Kinoshita, K, Hayashita-Kinoh, H, Nitahara-Kasahara, Y *et al.* (2009). Scalable purification of adeno-associated virus serotype 1 (AAV1) and AAV8 vectors, using dual ion-exchange adsorptive membranes. *Hum Gene Ther* **20**: 1013–1021.
42. Rohr, UP, Wulf, MA, Stahn, S, Steidl, U, Haas, R and Kronenwett, R (2002). Fast and reliable titration of recombinant adeno-associated virus type-2 using quantitative real-time PCR. *J Virol Methods* **106**: 81–88.
43. Engel, AG, Nagel, A, Walls, TJ, Harper, CM and Waisburg, HA (1993). Congenital myasthenic syndromes: I. Deficiency and short open-time of the acetylcholine receptor. *Muscle Nerve* **16**: 1284–1292.
44. Engel, AG and Santa, T (1971). Histometric analysis of the ultrastructure of the neuromuscular junction in myasthenia gravis and in the myasthenic syndrome. *Ann N Y Acad Sci* **183**: 46–63.
45. Engel, AG, Lindstrom, JM, Lambert, EH and Lennon, VA (1977). Ultrastructural localization of the acetylcholine receptor in myasthenia gravis and in its experimental autoimmune model. *Neurology* **27**: 307–315.
46. Otterness, IG and Chang, YH (1976). Comparative study of cyclophosphamide, 6-mercaptopurine, azathiopurine and methotrexate. Relative effects on the humoral and the cellular immune response in the mouse. *Clin Exp Immunol* **26**: 346–354.

Epilepsia, 53(1):79–86, 2012
doi: 10.1111/j.1528-1167.2011.03311.x

FULL-LENGTH ORIGINAL RESEARCH

Acute encephalopathy in children with Dravet syndrome

***Akihisa Okumura, †Mitsugu Uematsu, ‡George Imataka, §Manabu Tanaka, ¶Tohru Okanishi, #Tetsuo Kubota, **Akira Sudo, ††Jun Tohyama, ‡‡Megumi Tsuji, §§Iori Ohmori, ¶¶Misako Naiki, ¶¶Ayako Hiraiwa-Sofue, ##Hitoshi Sato, ***Shinji Saitoh, and *Toshiaki Shimizu**

***Department of Pediatrics, Juntendo University Faculty of Medicine, Tokyo, Japan; †Department of Pediatrics, Tohoku University School of Medicine, Sendai, Japan; ‡Department of Pediatrics, Dokkyo Medical University, Mibu, Japan; §Division of Neurology, Saitama Children's Medical Center, Saitama, Japan; ¶Department of Pediatrics, Seirei-Mikatahara General Hospital, Hamamatsu, Japan; #Department of Pediatrics, Anjo Kosei Hospital, Anjo, Japan; **Department of Pediatrics, Sapporo City General Hospital, Sapporo, Japan; ††Department of Pediatrics, Nishi-Niigata Chuo National Hospital, Niigata, Japan; ‡‡Division of Neurology, Clinical Research Institute, Kanagawa Children's Medical Center, Yokohama, Japan; §§Department of Physiology, Okayama University Graduate School of Medicine, Dentistry and Pharmaceutical Sciences, Okayama, Japan; ¶¶Department of Pediatrics, Nagoya University Graduate School of Medicine, Nagoya, Japan; ##Department of Pediatrics, Kanazawa Medical University School of Medicine, Uchinada, Japan; and ***Department of Pediatrics, Hokkaido University Graduate School of Medicine, Sapporo, Japan**

Summary

Purpose: The occurrence of acute encephalopathy in children with Dravet syndrome has been reported sporadically. This study clarified the features of acute encephalopathy in children with Dravet syndrome.

Methods: Through the mailing list of the Annual Zao Conference on Pediatric Neurology, we collected 15 patients with clinically diagnosed Dravet syndrome, who had acute encephalopathy, defined as a condition with decreased consciousness with or without other neurologic symptoms, such as seizures, lasting for >24 h in association with infectious symptoms.

Key Findings: There were seven boys and eight girls. A mutation of the *SCN1A* gene was present in nine (truncation in six and missense in three). The frequency of seizures during the 3 months before the onset of acute encephalopathy was monthly in seven children and none in three. The median age at the onset of acute encephalopathy was 44 months (range 8–184 months). All children had status epilepticus followed by coma as the initial manifestation. Two different distributions of brain lesions were observed on diffusion-weighted images during the acute phase: cerebral cortex–dominant lesions with or without deep gray matter involvement and subcortical-dominant lesions. Four children died; nine survived with severe sequelae, and two had moderate sequelae.

Significance: We must be aware that acute encephalopathy is an important complication in children with Dravet syndrome, and associated with fulminant clinical manifestations and a poor outcome.

KEY WORDS: Dravet syndrome, Acute encephalopathy, *SCN1A*, MRI.

Dravet syndrome is an epileptic syndrome characterized by the following: an onset with prolonged seizures that are often provoked by fever during early infancy, intractable seizures, repetitive episodes of status epilepticus (SE), and a subsequent decline in cognitive function (Dravet et al., 2005a). Fever sensitivity is an outstanding feature of Dravet syndrome. SE can be provoked by a febrile illness and may be followed by severe neurologic sequelae. Most patients with Dravet syndrome have a mutation in the *SCN1A* gene, which encodes the voltage-dependent sodium channel (Nav1.1) α subunit (Claes et al., 2001).

Acute encephalopathy, characterized by noninflammatory cerebral edema, implies sudden onset of severe central nervous system (CNS) symptoms such as convulsions followed by prolonged consciousness disturbance, and is often preceded by infection (Mizuguchi et al., 2007). In Japan, acute encephalopathy during influenza, exanthema subitum, and other febrile illnesses has attracted the attention of pediatric neurologists and general pediatricians since the outbreak of influenza-associated encephalopathy in the winter of 1997/1998 (Morishima et al., 2002). The occurrence of acute encephalopathy in children with Dravet syndrome has been reported sporadically in Japan (Takayanagi et al., 2010). In addition, we encountered several children with Dravet syndrome who had acute encephalopathy in association with a febrile illness. In addition, similar events have been reported from the developed countries in Europe, North America, and Oceania (Berkovic et al., 2006; Chipaux et al., 2010; Tang et al., 2011). Children with Dravet syndrome

Accepted September 14, 2011; Early View publication November 16, 2011.

Address correspondence to Akihisa Okumura, MD, Department of Pediatrics, Juntendo University, School of Medicine, 2-1-1 Hongo, Bunkyo-ku, Tokyo 113-8421, Japan. E-mail okumura@juntendo.ac.jp

complicated by acute encephalopathy were presented in the mailing list of the Annual Zao Conference on Pediatric Neurology. These children invariably had fulminant clinical course and poor outcome. The need for research on this topic was advocated.

We recruited children with Dravet syndrome who had acute encephalopathy through the mailing list of the Annual Zao Conference on Pediatric Neurology, to clarify the features of acute encephalopathy in children with Dravet syndrome. We present the results of a retrospective review of 15 patients.

Methods

We collected patients who met the following criteria through the mailing list of the Annual Zao Conference on Pediatric Neurology: clinical diagnosis of Dravet syndrome, a history of acute encephalopathy, and no evidence of direct CNS infection, such as bacterial meningitis, severe metabolic derangement, or other systemic disorders that could cause a reduction in consciousness. The mailing list of the Annual Zao Conference includes >500 pediatric neurologists from all over Japan. In February 2010, the chief author (AO) announced the enrollment of the patients with Dravet syndrome who had acute encephalopathy within the last 5 years. The chief author provided a structured research form on the mailing list. The members of the mailing list were asked to fill out the research form and to send it by email to the chief author if they had potential subjects. We did not request the responses from the members who did not have any potential subjects or would have difficulty participating in this study for any reasons. The 16 potential subjects were reported to the chief author from 14 hospitals until June 2010. After careful inspection of the chief author, 15 subjects were confirmed to meet the inclusion criteria. These 15 patients were a subject of this study. The clinical course of patient 11 was presented elsewhere as a case report (Tsuji et al., 2011). The approximate number of the patients with Dravet syndrome who were regularly followed was available from 12 hospitals. According to these data, acute encephalopathy was observed in 13 of approximately 170 children with Dravet syndrome. The number of patients with Dravet syndrome in each hospital ranged from 2–56.

The clinical diagnosis of Dravet syndrome was made according to the International League Against Epilepsy (ILAE) classification (Commission on Classification and Terminology of the International League Against Epilepsy, 1989). In this study, Dravet syndrome was diagnosed if all of the following characteristics were present: onset in the first year of life with hemiclonic or generalized seizures, frequent seizures provoked by fever, previously normal development, evolution of generalized spike-wave discharges, refractory to antiepileptic treatment, and subsequent delay in psychomotor development. Children without myoclonic seizures were included in the Dravet syndrome classification when they met all the characteristics described in the preceding. Acute encephalopathy was defined principally as a condition characterized by decreased consciousness with or without other neurologic findings, such as seizures, involuntary movement, and delirious behavior, lasting for >24 h in children with infectious symptoms including fever, cough, and diarrhea. However, barbiturate coma or continuous midazolam was administered in several patients. As to these patients, acute encephalopathy was diagnosed when prolonged coma was observed, even after the discontinuation of these drugs.

This study was approved by the institutional review board of Juntendo University Fac of Medicine. The patient's data were collected anonymously. Neuroimaging data were also collected after enrollment. We reviewed the clinical and neuroimaging features of the patients.

The outcomes of the patients were classified into the following four categories: mild sequelae (mild cognitive and/or motor impairment), moderate sequelae (moderate cognitive and/or motor impairment), severe sequelae (severe cognitive and/or motor impairment), and death. The severity of the cognitive impairment was classified according to the intelligence quotient or development quotient as follows: mild, 51–70; moderate, 30–50; and severe, <30. Intelligence quotient or developmental quotient was measured using Tsumori-Inage Developmental Assessment Test, Enjoji Analytical Development Test, KIDS Infant Development Scale, and Tanaka-Binet Intelligence Scales according to the age of the patient and the preference of each hospital. A formal assessment was not performed in some patients with apparently severe cognitive impairment. The severity of the motor impairment was classified into three groups: mild, if the patient could walk without support; moderate, if the patient could sit without support but could not walk without support; and severe, if the patient could not sit without support.

Results

Demographic data

The demographic data of the patients before the onset of acute encephalopathy are shown in Table 1. There were seven boys and eight girls. The onset of Dravet syndrome ranged from 2–7 months of age. All but one child had a history of SE before the onset of acute encephalopathy. A mutation in the *SCN1A* gene was present in 9 of the 12 children in whom a *SCN1A* mutation was examined, including multiplex ligation-dependent probe amplification: It was a truncation mutation in six children and a missense mutation in three. Myoclonic seizures were recognized in 14 children. Cognitive impairment before the onset of acute encephalopathy was absent in three children, mild in three, moderate in seven, and severe in two. The frequency of seizures during the 3 months before the onset of acute encephalopathy was monthly in seven children and none in three. Five children had histories of one or more episode of SE and three had a

Epilepsia, 53(1):79–86, 2012
doi: 10.1111/j.1528-1167.2011.03311.x

Table 1. Demographic features

Patient	Sex	Onset of DS (months)	*SCN1A* mutation	History of status epilepticus	Myoclonic Sz	CI before the onset of AE	Szs during 3 months before the onset of AE			AED at the onset of AE
							Frequency	Cluster	Status	
1	M	6	IVS 26-2 A>C	10	No	Moderate	None	0	0	VPA, CLB, KBr
2	F	3	L929del fsX934	Several	Yes	Moderate	Daily	0	0	VPA, CLB, CZP, KBr, ZNS, LTG
3	M	3	R568X	3	Yes	Moderate	Monthly	0	0	VPA, CZP, KBr
4	F	4	K1846fsX1856	15	Yes	Moderate	Weekly	0	1	VPA, ZNS, CLB
5	F	7	IVS4+1G>A	Several	Yes	None	Monthly	0	1	VPA, CZP
6	F	3	R701X	0	Yes	None	None	0	0	VPA, CZP, PB
7	M	2	A1339V	3	Yes	Mild	Monthly	1	0	VPA, ZNS, PB
8	F	4	Y145H	2	Yes	Moderate	Weekly	0	0	VPA, CZP
9	F	5	V1630L	1	Yes	Mild	None	0	0	VPA, CLB, KBr
10	F	6	None	4	Yes	Moderate	Weekly	1	0	VPA, CLB, PB, TPM
11	F	5	None	Frequent	Yes	Moderate	Monthly	0	4	VPA, CZP
12	M	4	None	3	Yes	None	Monthly	0	2	VPA
13	M	4	Not done	2	Yes	Severe	Weekly	1	0	VPA, CLB, PRM, SLT, AZA, ESM, CLZ
14	M	5	Not done	1	Yes	Severe	Monthly	0	0	VPA, ZNS, NZP
15	M	4	Not done	7	Yes	Mild	Monthly	0	4	VPA, CLB, ZNS

DS, Dravet syndrome; Sz, seizure; CI, cognitive impairment; AE, acute encephalopathy; SE, status epilepticus; VPA, valproate; CLB, clobazam; PB, phenobarbital; TPM, topiramate; PRM, primidone; SLT, sulthiame; AZA, acetazolamide; ESM, ethosuximide; CLZ, clorazepate; ZNS, zonisamide; NZP, nitrazepam; CZP, clonazepam; KBr, potassium bromide; LTG, lamotrigine.

Table 2. Acute encephalopathy and outcome

Patient	Onset of AE (months)	Prodromal illness	Pathogen	Duration of SE at the onset of AE	Treatment for the initial SE[a]	Maximum LOC	Outcome			
							Neurologic sequelae	Cognitive impairment	Motor impairment	Sz frequency after recovery
1	38	URI	ND	40 min	DZP	Coma	Severe	Severe	Severe	None
2	153	URI	ND	1 h	TP (2)	Coma	Severe	Severe	Severe	None
3	53	Flu	Flu A	4 h	DZP (2), PHT, TL, MDZ	Coma	Death			
4	45	URI	ND	50 min	DZP, MDZ	Coma	Severe	Severe	Severe	None
5	13	Subitum	HHV-6	1 h	MDZ	Coma	Severe	Severe	Severe	None
6	13	NSFI	ND	3 h	DZP, MDZ, PHT, PTB, TP	Coma	Death			
7	16	Subitum	ND	4 h	TL, MDZ (2), PB	Coma	Moderate	Mild	Moderate	Monthly
8	27	URI	ND	1.5 h	DZP, MDZ	Coma	Severe	Severe	Severe	None
9	45	URI	ND	50 min	DZP, MDZ	Coma	Moderate	Moderate	None	Monthly
10	61	URI	ND	2 h	MDZ (2), DZP (2)	Coma	Severe	Severe	Severe	None
11	15	URI	ND	2 h	DZP, MDZ, TL	Coma	Severe	Severe	Severe	None
12	8	URI	RSV	1 h	DZP (3), MDZ (3)	Coma	Severe	Severe	Severe	Monthly
13	92	URI	ND	1 h	DZP	Coma	Severe	Severe	Mild	Monthly
14	184	URI	ND	1 h	DZP (2), MDZ (4)	Coma	Death			
15	43	NSFI	ND	5 h	DZP, MDZ, PB, TP	Coma	Death			

AE, acute encephalopathy; LOC, loss of consciousness; Sz, seizure; Flu, influenza; URI, upper respiratory tract infection; Subitum, exanthema subitum; NSFI, nonspecific febrile illness; HHV-6, human herpesvirus 6; RSV, respiratory syncytial virus; DZP, diazepam; MDZ, midazolam; PB, phenobarbital; PHT, phenytoin; PTB, pentobarbital; TL, thiamylal; TP, thiopental.

[a]The AEDs until the cessation of SE are shown according to the order of administration. The numbers in the brackets indicate the number of the doses for each patient, when two or more doses were administered.

history of cluster seizures during the 3 months before the onset of acute encephalopathy. All children had been treated with antiepileptic drugs (AEDs), such as valproate, benzodiazepines, and bromide.

Acute encephalopathy

The clinical manifestations of the acute encephalopathy are shown in Table 2. The median age at the onset of acute encephalopathy was 44 months (range 8–184 months). Eleven children were younger than 5 years of age, whereas two were older than 10 years. All children had a febrile illness before the onset of acute encephalopathy. A pathogen was identified in three children: influenza A in one, human herpesvirus 6 in one, and respiratory syncytial virus in one. Rapid antigen test for influenza was negative in the other four children.

Neurologic findings of acute encephalopathy were characterized by a fulminant clinical course with SE and severe

Epilepsia, 53(1):79–86, 2012
doi: 10.1111/j.1528-1167.2011.03311.x

loss of consciousness. All children had SE followed by deep coma as the initial manifestation of acute encephalopathy. The duration of SE ranged from 40 min to 5 h. Although AEDs were administrated without a delay in a manner similar to that with the previous events with SE in most patients, seizures were refractory and persisted for 1 h or longer in 12 patients. More than two doses of AEDs were necessary to control SE in 12. Deep coma was seen following SE in all patients, even when seizures were controlled with one dose of AEDs. The loss of consciousness persisted for 2 weeks or longer in 13 children. Seizures were observed in all children on the first day, in seven on the second day, and in four on the third day. Thereafter, seizures were observed in only two children during the course of the acute encephalopathy. Although SE was seen on the first day in all patients, it was subsequently seen in only two children during the course of the acute encephalopathy. Delirious behavior was not seen in any child. No child had a biphasic clinical course: that is, an onset with SE, transient recovery of consciousness, and late clustering seizures with a worsening of consciousness. Despite the severe neurologic symptoms, serious systemic circulatory failure was not seen during the first few days after onset in any but one patient (Patient 15), even in those who died later. Vital signs such as heart rate, oximetry, blood pressure, and urine output were continuously monitored in all patients. Mild and transient hypotension was observed in some patients and was treated appropriately with catecholamine and volume expander.

The laboratory examinations on admission revealed thrombocytopenia (platelet count $<10.0 \times 10^4/\mu l$) in five (33%). Elevated levels of aspartate transaminase (>100 IU/L), alanine transaminase (>80 IU/L), lactate dehydrogenase (>600 IU/L), and creatine kinase (>400 IU/L) were present in seven (47%), three (20%), seven (47%), and three (20%), respectively. Elevated blood urea nitrogen (>20 mg/dl) and creatinine (>1.0 mg/dl) were seen in three (20%) and three (20%), respectively. Hypoglycemia (blood glucose <40 mg/dl) was not observed in any child, but hyperglycemia (blood glucose >200 mg/dl) was seen in three (20%). An elevated serum ammonia level was not seen in any child, whereas metabolic acidosis was present in six children (40%).

The neuroimaging findings are summarized in Table 3. Neuroimaging examinations were performed in 12 children during the first week. Three of them underwent computed tomography (CT) on the second day of illness, and marked brain edema was seen in all three. Magnetic resonance imaging (MRI) was performed in nine children and abnormal findings were seen in seven children. Two different distributions of brain lesions were observed on diffusion-weighted images: cerebral cortex-dominant lesions with or without deep gray matter involvement (Fig. 1A–D) and subcortical-dominant lesions (Fig. 1E,F). Five patients

Table 3. Neuroimaging findings

	Acute phase		Recovery phase	
Patient	Days after AE onset	Neuroimaging findings during the acute phase	Days after AE onset	Neuroimaging findings during the recovery phase
1	6	HIA in cerebral cortex, and caudate and lentiform nuclei on DWI	31	Diffuse atrophy on MRI
2	0	No abnormalities on MRI	10	HIA in cerebral cortex and corpus callosum on DWI
	4	HIA in cerebral cortex, caudate nuclei, thalami, and cerebellum on DWI		
3		Not done		Not done
4	0	HIA in cerebral cortex and subcortical WM on DWI	14	Diffuse atrophy on MRI
5	0	HIA in cerebral cortex, lentiform nuclei, and thalami on DWI	34	Diffuse atrophy on MRI
6	1	Marked brain edema on CT		Not done
7	0	No abnormalities on MRI	7	Mild atrophy on MRI
8	1	Marked brain edema on CT	68	Diffuse atrophy on MRI
9	0	HIA in subcortical WM on DWI	13	Mild atrophy on MRI
10		Not done	19	Mild atrophy, striatal necrosis on MRI
11		Not done	21	Diffuse atrophy on MRI
12	3	HIA in subcortical WM on DWI	21	Diffuse atrophy on MRI
13	1	No abnormalities on MRI	33	Diffuse atrophy on MRI
14	1	HIA in cerebral cortex, thalami, and cerebellum on DWI		Not done
15	1	Marked brain edema on CT		Not done

AE, acute encephalopathy; HIA, high intensity areas; WM, white matter; DWI, diffusion-weighted images; CT, computed tomography; MRI, magnetic resonance imaging.

Epilepsia, 53(1):79–86, 2012
doi: 10.1111/j.1528-1167.2011.03311.x

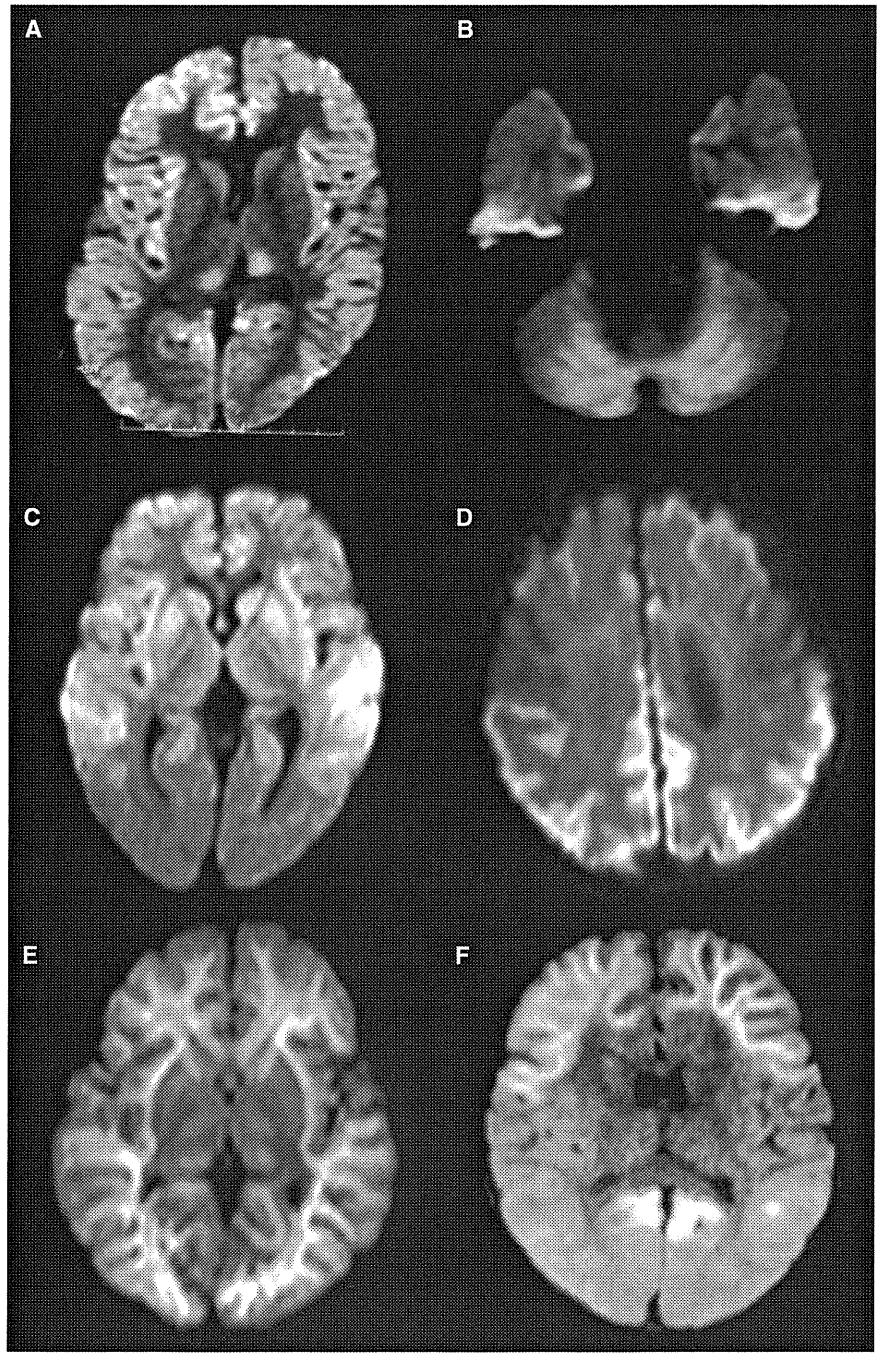

Figure 1.
Diffusion-weighted images. (**A**, **B**) Patient 15, 1 day after the onset of acute encephalopathy. Abnormal high intensities were observed in the cerebral cortex, thalami, and cerebellar hemispheres. (**C**) Patient 1, 6 days after the onset of acute encephalopathy. Abnormal high intensities were seen in the cortex in the frontotemporal region bilaterally and the caudate and lentiform nuclei bilaterally. (**D**) Patient 5, on the day of onset of acute encephalopathy. Abnormal high intensities were present in the cortex in the temporal-parietal-occipital region bilaterally. Slightly high intensities were also recognized in the cortex in the frontal region bilaterally. (**E**) Patient 12, 3 days after the onset of acute encephalopathy. Abnormal high intensities were seen in the entire subcortical white matter. (**F**) Patient 9, the day of the onset of acute encephalopathy. Abnormal high intensities were observed in the subcortical white matter in the frontal and mesial occipital regions bilaterally.

(Patients 1, 2, 4, 5, and 14) had cerebral cortex-dominant lesions. In addition to cortical lesions, caudate lesions were observed in two children, lentiform nuclei lesions in two, thalamic lesions in three, and cerebellar lesions in two. In three children, these lesions were present within the first 2 days after the onset. Two patients (Patients 9 and 12) had subcortical-dominant lesions: One patient had diffusion abnormalities in the entire subcortical white matter and the other had bilateral frontal lesions. No child with subcortical-dominant lesions had deep gray matter involvement. Among six children with cerebral cortex–dominant lesions, four had truncation mutations and one had no *SCN1A* mutation. *SCN1A* mutation was not assessed in the other two children. As to the two children with subcortical-dominant lesions, one had a missense mutation and the other had no *SCN1A* mutation. MRI after recovery from the acute encephalopathy was performed in 11 children. Marked, diffuse atrophy of the cerebral hemispheres was observed in seven children and mild atrophic changes in the other four.

Epilepsia, 53(1):79–86, 2012
doi: 10.1111/j.1528-1167.2011.03311.x

Regarding treatment, barbiturate coma was administered in 7 children and continuous midazolam infusion in 12 during the clinical course. Phenobarbital and phenytoin were used in two and three children, respectively. Artificial ventilation was required in 12 children. Steroid pulse therapy was performed in eight, steroid other than pulse therapy in four, and intravenous immunoglobulin in five. Selective or systemic hypothermia was applied in four children.

The outcome in these children was invariably poor (Table 2). Four children died; nine survived with severe sequelae and two had moderate sequelae. All but one surviving child had moderate or severe cognitive impairment, and nine had moderate or severe motor impairment. In contrast, the seizure frequency after recovery was reduced, compared with that before the onset of acute encephalopathy in most surviving patients. Seven children had no seizures after recovery and four had monthly seizures. Although no statistical analysis was performed because of the small number of children, the outcome was relatively worse in children with a truncation mutation than in those with a missense mutation. Of six children with truncation mutations, two died and the other four survived with severe sequelae. Of three children with missense mutations, moderate sequelae were seen in two and severe sequelae in one. Three children without *SCN1A* mutations had severe sequelae.

Discussion

Our study revealed that acute encephalopathy can be an important complication of Dravet syndrome. A catastrophic clinical course is the outstanding feature of acute encephalopathy in children with Dravet syndrome. Some authors have recently reported children with Dravet syndrome accompanied by acute encephalopathy (Chipaux et al., 2010; Takayanagi et al., 2010; Tang et al., 2011). The clinical course of these patients is characterized by severe SE, followed by massive neurologic regression and marked brain atrophy. These features are similar to those in our patients. Sakauchi et al. (2011) conducted a questionnaire survey on the causes and prevalence of deaths related to Dravet syndrome. They reported that acute encephalopathy with SE was the cause of mortality in 21 (36%) of 59 patients who died. Berkovic et al. (2006) found de novo mutations of *SCN1A* in 11 of 14 children with alleged vaccine encephalopathy. These patients may have had acute encephalopathy, like our patients. Moreover, Kobayashi et al. (2010) performed a mutational analysis of *SCN1A* in 15 children with various types of acute encephalopathy. A missense *SCN1A* mutation was detected in a patient with a history of acute encephalitis with refractory, repetitive partial seizures. These facts suggest that Dravet syndrome or *SCN1A* mutation may be a genetic predisposition of acute encephalopathy induced by infection.

We considered the catastrophic neurologic conditions in our patients as acute encephalopathy rather than severe SE, although it is well known that pyrexia can cause SE leading to severe neurologic sequelae or even death in children with Dravet syndrome (Oguni et al., 2001; Dravet et al., 2005a). The SE triggered by fever in children with Dravet syndrome is not usually followed by severe neurologic deterioration (Oguni et al., 2001; Dravet et al., 2005a,b). Postictal motor deficit may be observed in some patients after SE, but motor function usually recovers within a few hours. In contrast, our patients were characterized by severe neurologic deterioration and marked brain lesions on MRI. These neuroimaging abnormalities are distinct from those reported in Dravet syndrome including temporal sclerosis, nonspecific atrophic changes, and increased intensities in the white matter (Oguni et al., 2001; Dravet et al., 2005b; Siegler et al., 2005; Striano et al., 2007). Hypoxic ischemic damage in association with systemic circulatory failure may explain the widespread brain lesions. However, serious hypoxia and/or systemic circulatory failure were not observed in any but one patient during the first few days. On the other hand, SE and prolonged impairment of consciousness are core neurologic symptoms of acute encephalopathy induced by infectious diseases (Togashi et al., 2004; Nagao et al., 2008; Wada et al., 2009). Diffusion abnormalities on MRI are often observed in children with acute encephalopathy, even without serious hypoxia or systemic circulatory failure (Takanashi et al., 2006; Okumura et al., 2009). On the basis of these observations, we considered that the SE in our patients will be derived from acute encephalopathy in itself from the start of seizures, not from epilepsy.

We found two different patterns of diffusion abnormalities on MRI in our cohort: reduced diffusion in the cortex and deep gray matter and that in the subcortical white matter. The distribution of the diffusion abnormalities was unique in patients with cortical and deep gray matter involvement. Thalamic involvement is a remarkable feature of acute necrotizing encephalopathy (Mizuguchi, 1997). However, diffusion abnormalities of the cortex have not been reported in children with acute necrotizing encephalopathy. Studies of *scn1a* mRNA expression in mice have shown that *scn1a* mRNA is highly expressed in the thalami, deep cerebral nuclei, pons, medulla, and spinal cord (Ogiwara et al., 2007). The involvement of the caudate nuclei and putamen may be explained by high expression of the mutant *SCN1A*. Reduced diffusion in the subcortical white matter was observed in two of our patients. The distribution of diffusion abnormalities resembled that of acute encephalopathy with biphasic seizures and late reduced diffusion (AESD), proposed by Takanashi et al. (2006; Takanashi, 2009). However, biphasic clinical course, that is an outstanding feature of AESD, was not recognized in any of our patients. The different clinical manifestations despite similar MRI findings are difficult to explain at present.

The precise incidence of acute encephalopathy among children with Dravet syndrome is not easy to determine. In our study, 13 of approximate 170 children with Dravet

Epilepsia, 53(1):79–86, 2012
doi: 10.1111/j.1528-1167.2011.03311.x

syndrome had acute encephalopathy. Although this result can be largely overestimated, the incidence of acute encephalopathy among children with Dravet syndrome will be more frequent than that among general children. It is estimated that acute encephalopathy develops in 500–1,000 among 17 million children every year in Japan. These facts indicate that children with Dravet syndrome will be at an increased risk for acute encephalopathy.

It is remarkable that the seizure frequency before the onset of acute encephalopathy was relatively low in a majority of our patients. Three children had no seizures and seven had monthly seizures during the 3 months before the onset of encephalopathy. Given the refractory nature of Dravet syndrome, antiepileptic drug treatment was appropriate in our patients because of lower seizure frequency. We must be aware that acute encephalopathy can develop in children with Dravet syndrome unexpectedly, even if the seizures are well controlled by AEDs.

The neuroimaging findings and the severity of the sequelae in our children may be related to the type of *SCN1A* mutation, although statistical analyses could not be performed because of the small sample size. Children with truncation *SCN1A* mutations tended to have cerebral cortex–dominant lesions and a poor outcome. Those with no mutation or a missense mutation tended to have subcortical-dominant lesions with a relatively favorable outcome. This suggests that children with a truncation *SCN1A* mutation may develop more severe acute encephalopathy. There is an ongoing controversy on the genotype–phenotype correlation of *SCN1A* mutations. Further studies with more patients are necessary to clarify the relationship between the type of *SCN1A* mutation and the severity of acute encephalopathy.

Recent genetic studies have revealed that the mutation in the *PCDH19* gene encoding protocadherin 19 is present in some female patients with Dravet syndrome (Depienne et al., 2009; Marini et al., 2010). The patients with Dravet syndrome with *PCDH19* mutations share most of the hallmark features of Dravet syndrome with *SCN1A* mutation including early onset, seizures provoked by fever, frequent SE, and stagnation of development (De Jonghe, 2011). The relation between acute encephalopathy and *PCDH19* mutation will be a subject of future studies.

Fever-induced refractory epileptic encephalopathy in school-aged children (FIRES) is a recently proposed clinical entity (Nabbout et al., 2011). Acute phase of FIRES is characterized by seizures rapidly aggravating into SE a few days to 1 week after febrile illness. Severe seizures and poor outcome are similar between FIRES and acute encephalopathy in children with Dravet syndrome. However, there are some differences between these two conditions. Onset in most children with FIRES is after fever had disappeared, whereas onset of encephalopathy is usually associated with fever in children with Dravet syndrome. Although repeated seizures up to 100 per day are common in children with FIRES, a long seizure refractory against AEDs is characteristic in acute encephalopathy in children with Dravet syndrome. FIRES usually occurs in previously healthy children, but a delay in psychomotor development is not uncommon prior to acute encephalopathy in children with Dravet syndrome. Therefore, these two clinical entities will be distinguishable.

In conclusion, we reviewed the clinical and neuroimaging features of acute encephalopathy in 15 children with Dravet syndrome. The acute encephalopathy was characterized by fulminant manifestations with SE and subsequent deep coma. Diffusion-weighted images revealed two different patterns of brain lesions: cerebral cortical–dominant lesions and subcortical-dominant lesions. The outcome was mostly poor, with death or severe neurologic sequelae.

Acknowledgments

This study is supported by the grants from the Ministry of Health, Labour, and Welfare of Japan (H21-Shinkou-Ippan-010 and H22-Nanji-Ippan-049), and the grants from the Ministry of Education, Culture, Sports, Science and Technology of Japan (20249053 and 23591518).

Disclosure

None of the authors has any conflict of interest to disclose. We confirm that we have read the Journal's position on issues involved in ethical publication and affirm that this report is consistent with those guidelines.

References

Berkovic SF, Harkin L, McMahon JM, Pelekanos JT, Zuberi SM, Wirrell EC, Gill DS, Iona X, Mulley JC, Scheffer IE. (2006) De-novo mutations of the sodium channel gene SCN1A in alleged vaccine encephalopathy: a retrospective study. *Lancet Neurol* 5:488–492.

Chipaux M, Villeneuve N, Sabouraud P, Desguerre I, Boddaert N, Depienne C, Chiron C, Dulac O, Nabbout R. (2010) Unusual consequences of status epilepticus in Dravet syndrome. *Seizure* 19:190–194.

Claes L, Del-Favero J, Ceulemans B, Lagae L, Van Broeckhoven C, De Jonghe P. (2001) De novo mutations in the sodium-channel gene SCN1A cause severe myoclonic epilepsy of infancy. *Am J Hum Genet* 68:1327–1332.

Commission on Classification and Terminology of the International League Against Epilepsy. (1989) Proposal for revised classification of epilepsies and epileptic syndromes. *Epilepsia* 30:389–399.

De Jonghe P. (2011) Molecular genetics of Dravet syndrome. *Dev Med Child Neurol* 53(Suppl.):7–10.

Depienne C, Bouteiller D, Keren B, Cheuret E, Poirier K, Trouillard O, Benyahia B, Quelin C, Carpentier W, Julia S, Afenjar A, Gautier A, Rivier F, Meyer S, Berquin P, Hélias M, Py I, Rivera S, Bahi-Buisson N, Gourfinkel-An I, Cazeneuve C, Ruberg M, Brice A, Nabbout R, Leguern E. (2009) Sporadic infantile epileptic encephalopathy caused by mutations in PCDH19 resembles Dravet syndrome but mainly affects females. *PLoS Genet* 5:e1000381.

Dravet C, Bureau M, Oguni H, Fukuyama Y, Cokar O. (2005a) Severe myoclonic epilepsy in infancy (Dravet syndrome). In Roger J, Bureau M, Dravet C, Genton P, Tassinari CA, Wolf P (Eds) *Epileptic syndromes in infancy, childhood and adolescence*. 4th ed. John Libbey Eutotext, London, pp. 89–113.

Dravet C, Bureau M, Oguni H, Fukuyama Y, Cokar O. (2005b) Severe myoclonic epilepsy in infancy: Dravet syndrome. In Delgado Escueta AV, Guerrini R, Medina MT, Genton P, Bureau M, Dravet C (Eds) *Advances in Neurology*, vol. 95. Lippincott Williams and Wilkins, Philadelphia, pp. 71–102.

Kobayashi K, Ouchida M, Okumura A, Maegaki Y, Nishiyama I, Matsui H, Ohtsuka Y, Ohmori I. (2010) Genetic seizure susceptibility underlying acute encephalopathies in childhood. *Epilepsy Res* 91:143–152.

Marini C, Mei D, Parmeggiani L, Norci V, Calado E, Ferrari A, Moreira A, Pisano T, Specchio N, Vigevano F, Battaglia D, Guerrini R. (2010) Protocadherin 19 mutations in girls with infantile-onset epilepsy. *Neurology* 75:646–653.

Mizuguchi M. (1997) Acute necrotizing encephalopathy of childhood: a novel form of acute encephalopathy prevalent in Japan and Taiwan. *Brain Dev* 19:81–92.

Mizuguchi M, Yamanouchi H, Ichiyama T, Shiomi M. (2007) Acute encephalopathy associated with influenza and other viral infections. *Acta Neurol Scand Suppl* 186:45–56.

Morishima T, Togashi T, Yokota S, Okuno Y, Miyazaki C, Tashiro M, Okabe N. (2002) Collaborative Study Group on Influenza-Associated Encephalopathy in Japan. Encephalitis and encephalopathy associated with an influenza epidemic in Japan. *Clin Infect Dis* 35: 512–517.

Nabbout R, Vezzani A, Dulac O, Chiron C. (2011) Acute encephalopathy with inflammation-mediated status epilepticus. *Lancet Neurol* 10:99–108.

Nagao T, Morishima T, Kimura H, Yokota S, Yamashita N, Ichiyama T, Kurihara M, Miyazaki C, Okabe N. (2008) Prognostic factors in influenza-associated encephalopathy. *Pediatr Infect Dis J* 27:384–389.

Ogiwara I, Miyamoto H, Morita N, Atapour N, Mazaki E, Inoue I, Takeuchi T, Itohara S, Yanagawa Y, Obata K, Furuichi T, Hensch TK, Yamakawa K. (2007) Na(v)1.1 localizes to axons of parvalbumin-positive inhibitory interneurons: a circuit basis for epileptic seizures in mice carrying an scn1a gene mutation. *J Neurosci* 27:5903–5914.

Oguni H, Hayashi K, Awaya Y, Fukuyama Y, Osawa M. (2001) Severe myoclonic epilepsy in infants – a review based on the Tokyo Women's Medical University series of 84 cases. *Brain Dev* 23:736–748.

Okumura A, Kidokoro H, Tsuji T, Suzuki M, Kubota T, Kato T, Komatsu M, Shono T, Hayakawa F, Shimizu T, Morishima T. (2009) Differences of clinical manifestations according to the patterns of brain lesions in acute encephalopathy with reduced diffusion in the bilateral hemispheres. *Am J Neuroradiol* 30:825–830.

Sakauchi M, Oguni H, Kato I, Osawa M, Hirose S, Kaneko S, Takahashi Y, Takayama R, Fujiwara T. (2011) Retrospective multiinstitutional study of the prevalence of early death in Dravet syndrome. *Epilepsia* 52:1144–1149.

Siegler Z, Barsi P, Neuwirth M, Jerney J, Kassay M, Janszky J, Paraicz E, Hegyi M, Fogarasi A. (2005) Hippocampal sclerosis in severe myoclonic Epilepsy in Infancy: a retrospective MTI Study. *Epilepsia* 45:704–708.

Striano P, Mancardi MM, Biancheri R, Madia F, Gennaro E, Paravidino R, Beccaria F, Capovilla G, Dalla Bernardina B, Darra F, Elia M, Giordano L, Gobbi G, Granata T, Ragona F, Guerrini R, Marini C, Mei D, Longaretti F, Romeo A, Siri L, Specchio N, Vigevano F, Striano S, Tortora F, Rossi A, Minetti C, Dravet C, Gaggero R, Zara F. (2007) Brain MRI findings in severe myoclonic epilepsy in infancy and genotype–phenotype correlations. *Epilepsia* 48:1092–1096.

Takanashi J. (2009) Two newly proposed infectious encephalitis/encephalopathy syndromes. *Brain Dev* 31:521–528.

Takanashi J, Oba H, Barkovich AJ, Tada H, Tanabe Y, Yamanouchi H, Fujimoto S, Kato M, Kawatani M, Sudo A, Ozawa H, Okanishi T, Ishitobi M, Maegaki Y, Koyasu Y. (2006) Diffusion MRI abnormalities after prolonged febrile seizures with encephalopathy. *Neurology* 66:1304–1309.

Takayanagi M, Haginoya K, Umehara N, Kitamura T, Numata Y, Wakusawa K, Hino-Fukuyo N, Mazaki E, Yamakawa K, Ohura T, Ohtake M. (2010) Acute encephalopathy with a truncation mutation in the SCN1A gene: a case report. *Epilepsia* 51:1886–1888.

Tang S, Lin JP, Hughes E, Siddiqui A, Lim M, Lascelles K. (2011) Encephalopathy and SCN1A mutations. *Epilepsia* 52:e26–e30.

Togashi T, Matsuzono Y, Narita M, Morishima T. (2004) Influenza-associated acute encephalopathy in Japanese children in 1994–2002. *Virus Res* 103:75–78.

Tsuji M, Mazaki E, Ogiwara I, Wada T, Iai M, Okumura A, Yamashita S, Yamakawa K, Osaka H. (2011) Acute encephalopathy in a patient with Dravet syndrome. *Neuropediatrics* 42:78–81.

Wada T, Morishima T, Okumura A, Tashiro M, Hosoya M, Shiomi M, Okuno Y. (2009) Differences in clinical manifestations of influenza-associated encephalopathy by age. *Microbiol Immunol* 53:83–88.